REACTION RATE STUDIES IN A TRICKLE - BED REACTOR

A Thesis Submitted
in Partial Fulfilment of the Requirements
for the Degree of
MASTER OF TECHNOLOGY

by

DOMMETI SANDRA MARY SUJATHA

to the

DEPARTMENT OF CHEMICAL ENGINEERING
INDIAN INSTITUTE OF TECHNOLOGY KANPUR
February 1994

CHE-1994-M-SUJ-REA

CERTIFICATE

This is certify that the present work entitled "REACTION RATE STUDIES IN A TRICKLE-BED REACTOR" has been carried out by Miss Dommeti Sandra Mary Sujatha under my supervision and has not been submitted elsewhere for a degree.

M. Someswara Rao

Professor

Department of Chemical Engineering

IIT Kanpur

Dated: February, 1994.

ACKNOWLEDGEMENTS

I wish to express my deep sense of gratitude and indebtedness to my supervisor Professor M.S. Rao for his valuable guidance, enthusiastic support and constant encouragement at each stage of the work.

I take this opportunity to express my sincere gratitude to Professor D.P. Rao for his encouragement, stimulating discussions and valuable suggestions at all stages of this work.

I gratefgully acknowledge the financial assistance provided by Engineers India Ltd.,New Delhi in the form of an EIL scholarship. Acknowledgements are due to Department of Science and Technology for providing part of the project equipment (DST/ChE/9243). Activated carbon catalyst was provided by Calgon Carbon Corporation, Pittsburgh, Pa., USA.

I wish to express my indebtedness to Prof.D.N. Dhar, Prof.S. Sarkar, Prof.V. Chandrasekhar for their helpful discussions.

I am thankful to Mr.P.V. Ravindra for his cooperation and helpful discussions at all stages of this work. I am thankful to Mr.S. Subramanyam for all his help and to Mr.S.L. Yadav for his typing.

I am grateful to the staff of Chemical Engineering Workshop and Unit Operations Laboratory without whose help this work would not have been successful.

Thanks are due to all student friends who have contributed to my cherished stay at IIT Kanpur.

D.S.M. Sujatha

CONTENTS

LIST OF FIGURES

LIST OF TABLES

ABSTRACT

Trickle-bed reactors present several intriguing aspects, viz., a minimum in the reaction rate with liquid flow rate, hysteresis in gas-phase pressure drop, flickering hot spots etc. Recently, it has been demonstrated that the flow texture in non-prewetted and prewetted trickle-beds is different. A close scrutiny of the literature reveals that adequate attention has not been paid to the mode of operation in reaction rate measurements. In the present work, experimental studies were carried out to examine the reaction rate behavior of the prewetted and non-prewetted beds.

Experiments were conducted on a bed with a rectangular cross-section of 8cm x 6cm. A special grid enabled the collection of liquid from sixteen equally sized sections to obtain the liquid flow distribution. Oxidation of sulfur dioxide over activated carbon was used as a model reaction system. Reaction rates were measured for prewetted and non-prewetted beds.

In case of non-prewetted beds at very low liquid flow rates, 20% of the bed was found to be occupied with dry zones. The liquid flow through the rest of the bed ~~being~~ was predominantly filament flow. In case of prewetted beds, the liquid was flowing throughout the bed cross-section. The liquid distribution was more uniform in prewetted beds compared to that in non-prewetted beds at low liquid flow rates. However, at higher liquid flow rates, ~~the liquid flow rates~~, the liquid flow distribution was found to be similar in both prewetted and non-prewetted beds.

The studies revealed that the reaction rates decreased with increase in liquid flow rate for prewetted beds. A model has been developed to fit the experimental data obtained in prewetted mode of operation. The model parameters, viz., gas-liquid and liquid-solid mass transfer coefficients were estimated from the experimental data assuming complete wetting of the catalyst particles.

CHAPTER 1

INTRODUCTION AND LITERATURE SURVEY

I.1 Introduction

Trickle-bed reactors are three-phase reactors with cocurrent down flow of gas and liquid through a fixed bed of catalyst particles. These reactors are used in the chemical, petrochemical and petroleum industries, as well as in waste water treatment. Some of the well known applications in chemical processing are- oxidation of sulfur dioxide, formic acid, acetic acid and ethanol; hydrogenation of α-methylstyrene, cyclohexane, benzene and crotonaldehyde; hydrodesulfurization of petroleum fractions and synthesis of 2-butyne-1,4-diol from acetylene and formaldehyde.

Trickle-bed reactors are physically similar to the packed bed absorption columns. The major differences are as follows:

(1) In absorbers, the packing is an inert, non-porous material, which has the main purpose of improving the gas-liquid contacting, while in trickle beds, the packing is an active porous catalyst that could be in the form of spherical, cylindrical or granular pellets.

(2) Packed absorbers are operated at fairly high gas and liquid velocities, while trickle beds are operated at low gas and liquid velocities.

Several advantages associated with trickle-bed reactors as compared to other types of three-phase reactors include:

(i) the flow patterns that approach plug-flow;

(ii) high catalyst loading per unit volume of the liquid;

(iii) low energy dissipation rate (an order of magnitude lower

than for slurry reactors);

(iv) much greater flexibility with respect to the production rates and operating conditions used.

The reactor with cocurrent upflow operation of both gas and liquid is referred to as the packed bubble-bed reactor. The pressure drop in down flow operation (in trickle-bed reactors) is less than that for upflow reactors (like packed bubble-bed reactors) thus reducing the pumping energy costs. The contribution of homogeneous liquid-phase side reactions which can be significant in some cases in packed bubble-bed reactors is relatively small in trickle-bed reactors due to lower liquid holdup. Because of the absence of flooding cocurrent down flow is the most common mode of operation in industry. However, trickle-bed reactors cannot be used for highly exothermic reactions and are impracticable for systems with rapidly deactivating catalysts. Also when these reactors are operated at low liquid rates, part of the catalyst may not be wetted and may only be exposed to the gas phase reactant. This can lead to complications such as hot spot formation, temperature run-away and poorer utilization of the catalyst, whereas in a packed bubble-bed reactor, the catalyst is completely wetted and these complications will not exist. Heat transfer efficiency and heat removal are better in packed bubble bed reactors due to larger liquid holdup and liquid velocity than in trickle bed reactors.

The superficial liquid velocities encountered in trickle beds range from 0.01 to 0.3 cm/s in pilot plant reactors and from 0.1 to 2 cm/s in commercial reactors. The superficial gas velocity

ranges from 2 to 45 cm/s in pilot plant reactors and from 15 to 300 cm/s in commercial reactors. These are indicative ranges of flow rates and not definitive. Depending on the gas and liquid flow rates and the physical properties of the liquid, wetting properties of the solid, and nature of the porous structure in the packed bed, various flow regimes may exist in a trickle bed. A knowledge of this is essential in understanding the hydrodynamics and mass transfer characteristics. Sato et al. (1973) observed the various flow regimes in cocurrent downflow in packed beds using glass spheres of 2.59 - 16.5 mm diameter. They classified these flow regimes into three distinct flow patterns.

(a) At a low liquid rate, the flow pattern is trickling, where the liquid trickles over the packing essentially in a laminar flow. Here the flow in one phase is not significantly affected by the flow in the other phase and is known as a low-interaction regime.

(b) At higher gas and/or liquid rates the interaction between the gas and liquid phases is rather high and is known as a high interaction regime or pulsing flow.

(c) At very high liquid rates greater than 3 cm/s and low gas rates, the liquid becomes the continuous phase and the gas flows as a dispersed phase in the form of bubbles. This is referred to as the dispersed bubble flow regime.

The phenomenological picture, based on experimental evidence is as follows. Upto moderate gas velocities ($G < 1$ kg/m^2.s) and low liquid velocities ($L < 5$ kg/m^2.s) trickle-flow always persists. In this regime the gas flows as a continuous phase

through the bed and the liquid flows in the form of films. In this regime at a fixed gas velocity, as the liquid velocity is increased from transition to pulsing flow, only at very low gas velocities ($G < 0.01$ kg/m^2.s) can a transition to a dispersed bubble flow take place.

In dispersed-bubble flow the continuous liquid phase drags along the discrete gas bubbles. Pulsing flow is characterized by alternating flow of gas-rich and liquid-rich slugs which normally lead to noticeable pressure fluctuations in the bed and oscillations in the measured pressure drop. At a fixed liquid velocity in the trickle flow regimes, an increase in gas velocity also eventually leads from trickle to pulsing flow unless the liquid velocity is so low ($L < 5$ kg/m^2.s) that transition to spray flow occurs instead. In spray flow liquid droplets are carried by a continuous gas stream.

In view of its commercial significance, many studies have been performed to understand the performance of trickle beds. A better understanding of the distribution of the gaseous and liquid phases is of special interest as it controls the other transport processes and thus the overall reactor performance. Phase distribution at the reactor scale is expressed in the form of various flow regimes - trickling, pulsing, bubble and spray flows. Most common in practice is the trickling flow that occurs at moderate liquid and gas flow rates. In this regime, the liquid flows down the bed from particle to particle on the surface of the packings while the gas travels in the interstitial void space. The trickling regime can be further divided into two regimes. At

sufficiently low liquid flow rates, a fraction of the packings remain unwetted. This is the partial wetting trickling regime. If the liquid flow rate is increased, the partial wetting regime changes to complete wetting trickling regime in which the packings are totally wetted by the liquid.

In the trickling regime, some interesting flow features at the particle scale can be identified. The liquid holdup comprises films, rivulets, pendular structures, liquid pockets and filaments (Fig. 1). Films and rivulets are associated with a single particle, while other flow features involve two or more particles. A rivulet is a liquid stream flowing over the surface of a particle and can result from the splitting of a liquid film on the surface of a catalytic particle. A pendular structure resides at the contact point of two pellets while a liquid pocket extends over several pore chambers. The shape of a liquid pocket is random and depends on the configuration of the packings at a given location within the bed. Filaments are liquid streams that flow down the bed in the channels between the particles. The lateral width of a filament can extend over more than one pore chamber. A filament can be viewed as a continuous string of liquid pockets. The relative amounts of these features are expected to vary with the gas and liquid flow rates, surface tension, wettability, the gas and liquid inlet distributors used, and the size and shape of the packings, among other physical parameters and operating conditions. Also as reported by Lutran et al. the flow pattern is expected to depend on whether the bed has been prewetted by flooding the column with liquid or initially dry.

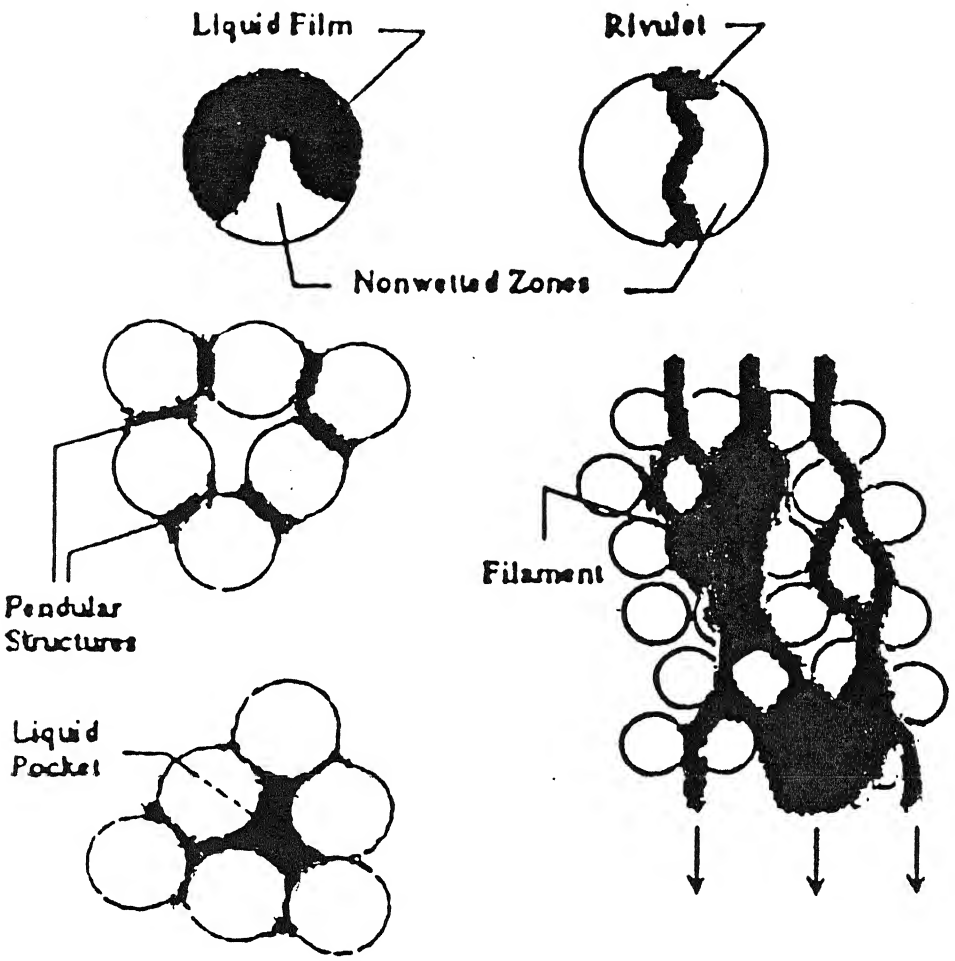

Fig.1 Flow features in the trickling regime: a liquid film, a rivulet, pendular structures, a liquid pocket and a filament. A film can completely or partially wet the sphere. A rivulet can be considered to be a narrow film. While pendular structures reside at the contact point between two pellets, a liquid pocket fills the inter-particle pore space formed by more than two spheres. A filament is a stream of liquid flowing down the bed. It can be considered to be a string of liquid pockets.

The objective of this work is to experimentally observe the effect of start up procedure (initially dry bed and prewetted by flooding) on the liquid flow distribution and also on the reaction rates. Oxidation of SO_2 over activated carbon catalyst is chosen as the model reaction system. In particular the effect of startup procedure on the rate of SO_2 oxidation at different superficial liquid velocities at a particular gas velocity are studied.

1.2 Literature Survey

1.2.1 Literature Survey on Liquid Flow Distribution Measurements

Because of the absence of suitable experimental techniques, studies of liquid distribution were limited to two macroscopic quantities - liquid holdup and wetting efficiency. Liquid holdup is defined as the volume of liquid per unit volume of bed. It can be divided into two parts: internal and external holdup. Internal holdup refers to the liquid held within the catalyst particles by capillary action and external holdup to the interparticle liquid. A large number of correlations have been proposed for liquid holdup and are summarized by Gianetto et al. (1978). Also frequently reported is the residual holdup, which is the fraction of liquid that remains after the reactor has been flooded with liquid and then drained.

Another measure of liquid distribution is the wetting efficiency. It is the fraction of external surface area of the catalyst particles that is covered by the liquid. However, the liquid holdup and wetting efficiency are not expected to be uniform within a trickle bed randomly packed with catalyst

particles. Indeed, very little is known about the actual flow pattern within the bed. Christensen et al. (1986) studied the pressure drop hysteresis observed in the cocurrent downflow of air and water under trickling flow regime. For given gas and liquid flow rates, the magnitude of the pressure gradient does not have a unique value. The observed maximum pressure drop can be more than twice the minimum pressure drop under identical operating conditions. They concluded that the multiplicity of pressure drops or equivalently hydrodynamic states, is caused by the existence of two different modes of flow, viz., film flow and filament flow. The former leads to a higher pressure drop because of the more vigorous interactions between the gas and liquid phases. They were able to see these two different patterns through the plexiglas walls of thin column, packed with 3 mm glass spheres. Their observation, however, was confined to the immediate proximity of the walls, and the interior of the bed remained unreachable.

An experiment was carried out by Melli (1989) to better understand the particle scale flow features. He concluded that flow pattern at the reactor scale such as the different flow regimes, is a result of the microscopic flow characteristics at the particle level.

Herskowitz and Smith (1978) measured the liquid flow distribution at the bottom of the bed employing four annular rings. They observed that the liquid distribution is uniform for aspect ratios greater than 18 for porous particles of 0.26 to 1.11 cm size. Ahtchi-Ali and Pedersen (1986) have passed HNO_3 solution

over the packing, composed of copper cylinders of 1.0 cm in diameter and length. The weight loss for every cylinder is noted. Considering ~~heat~~ that the weight loss of a particle is proportional to its irrigation rate, they obtained the histograms of the particle irrigation rate. They found that the irrigation rate was not uniform in the bed. Marchot et al. (1992) measured the liquid flow distribution on a laboratory trickling filter, packed with cylinders of polymeric material of 5.0 cm x 3.0 cm size; rather very large size compared to the particles in trickle-bed reactors. The histograms of fraction of the cross-sectional area with flow rates were obtained. The histograms reveal that about half the bed cross-section is not receiving liquid and flow rate distribution is not uniform in the rest of the bed cross section. Bemer and Zuiderweg (1978) studied the radial distribution of liquid employing glass raschig rings of 1.0, 2.0 and 3.0 cm size. They employed a single liquid inlet and found that most of the liquid is passing through the central region of the bed. Except for the studies by Herskowitz and Smith, the particle sizes employed in these studies are too large compared to those normally employed in trickle-bed reactor.

Lutran et al. (1991) studied the liquid distribution with a stagnant gas phase, employing the Computer Aided Tomography (CAT). They observed that the liquid distribution over glass beads in non-prewetted and prewetted beds was entirely different. Lazzaroni et al. (1988) developed a technique to determine the extent of external wetting of the catalyst particles. The particles were colored by a coloring reactant introduced in the

liquid phase and the extent of wetting was estimated by measuring the color intensity of the particles. By employing a point liquid source and annular collectors, the liquid distribution over the particles was measured. They observed that the liquid distribution is uniform across the bed and the extent of wetting of the catalyst particles in non-prewetted and prewetted beds is different. The particle wetting of the particles varied from 0.6 to 0.8 and 0.3 to 0.5 in prewetted and non-prewetted beds, respectively.

At present, the modelling of trickle-bed reactors is based on the assumption that the catalyst particles are externally partially wetted and the liquid distribution is uniform across the bed. However, the extent of wetting of the catalyst was ascertained from reaction rate data. But there is no direct evidence of partial wetting in a trickle-bed reactor except for the work of Lazzaroni et al. (1988). It is the object of the present study to study the effect of startup procedure on the reaction rates. Oxidation of SO_2 is taken as a model reaction, the literature on which briefly reviewed below.

1.2.2 Literature Survey on SO_2 Oxidation in Trickle Bed Reactors

The idea of recovering SO_2 from gases by oxidation to SO_3 over dry catalysts has received considerable attention from the discovery that activated carbon is one of the best catalysts for the oxidation of SO_2 (Davtyan and Ovchinikova, 1955). From the view point of the cost per unit mass of catalyst, activated carbon appears to be highly attractive economically. However, the rate of SO_2 oxidation over activated carbon abruptly decreases when the

oxidation product, which will not desorb spontaneously at room temperature, has occupied all of the active sites on the dry carbon surface. It was suggested by Hartman and Coughlin (1972) that water be used to remove the SO_3 from the catalyst surface by using trickle bed reactors for this reaction.

Various authors have studied different aspects of SO_2 oxidation in trickle bed reactors. Hartman and Coughlin (1971) studied the steady-state, continuous, countercurrent contacting of SO_2-bearing air with water in a column packed with carbon and modelled the reaction by combining the classical treatment for gas absorption with expressions for the rate of transport through the liquid and for the rate of catalytic oxidation of SO_2 within the porous carbon. Pavko and Levec (1981) studied the trickle-bed reactor performance by employing this reaction and determined the fraction of particle surface effectively wetted by liquid by making differential reactor measurements. He also concluded that a relatively deeper catalyst bed of approximately uniform liquid distribution can be attained by using the inert prepacking and also that a simple partial wetting model describes the behavior of a laboratory trickle-bed reactor well. Berruti et al. (1984) studied this reaction in a laboratory-scale trickle-bed reactor to develop empirical models describing the reactor behaviour. They developed two different models to interpret the experimental data - one considering that the external area of the catalyst is divided into two zones (wetted and dry) both active with respect to mass transfer; the other assuming that only one zone of the external area involves mass transfer and that the mass transfer

coefficient must be calculated according to film theory.

Mata and Smith (1981) also studied this reaction and observed that the reaction rate has a minimum value at an intermediate liquid flow for both saturated and unsaturated liquid feeds. They also presented a method for analyzing experimental, integral reactor data to determine rate parameters, including the wetting fraction in trickle beds. For the same catalyst and virtually identical experimental units and procedures, the rates measured by Mata and Smith (1981) rise as the liquid flow rate drops, whereas the rates obtained by Berruti et al. (1981) drop as shown in Fig.2. Pavko and Levec (1981) employing a G32 activated carbon did not observe a minimum nor did Hartman and Coughlin (1972). The latter investigators used a countercurrent trickle bed and a NAG (North American Carbon Inc.) activated carbon. Other experimental studies on SO_2 oxidation in a trickle bed did not systematically examine the effect of liquid flow rate.

Minima in the reaction rate vs superficial velocity curves have been reported for other trickle bed reactor systems. Sedricks and Kenney (1973) working with the hydrogenation of crotonaldehyde on a supported palladium catalyst, Satterfield and Ozel (1973) studying the hydrogenation of benzene, and Herskowitz and Mosseri (1983) using the hydrogenation of α-methyl styrene observed that decreasing the wetting (by decreasing the liquid flow rate) increased the rate of hydrogenation. This phenomenon is cited as the source of the rate minimum.

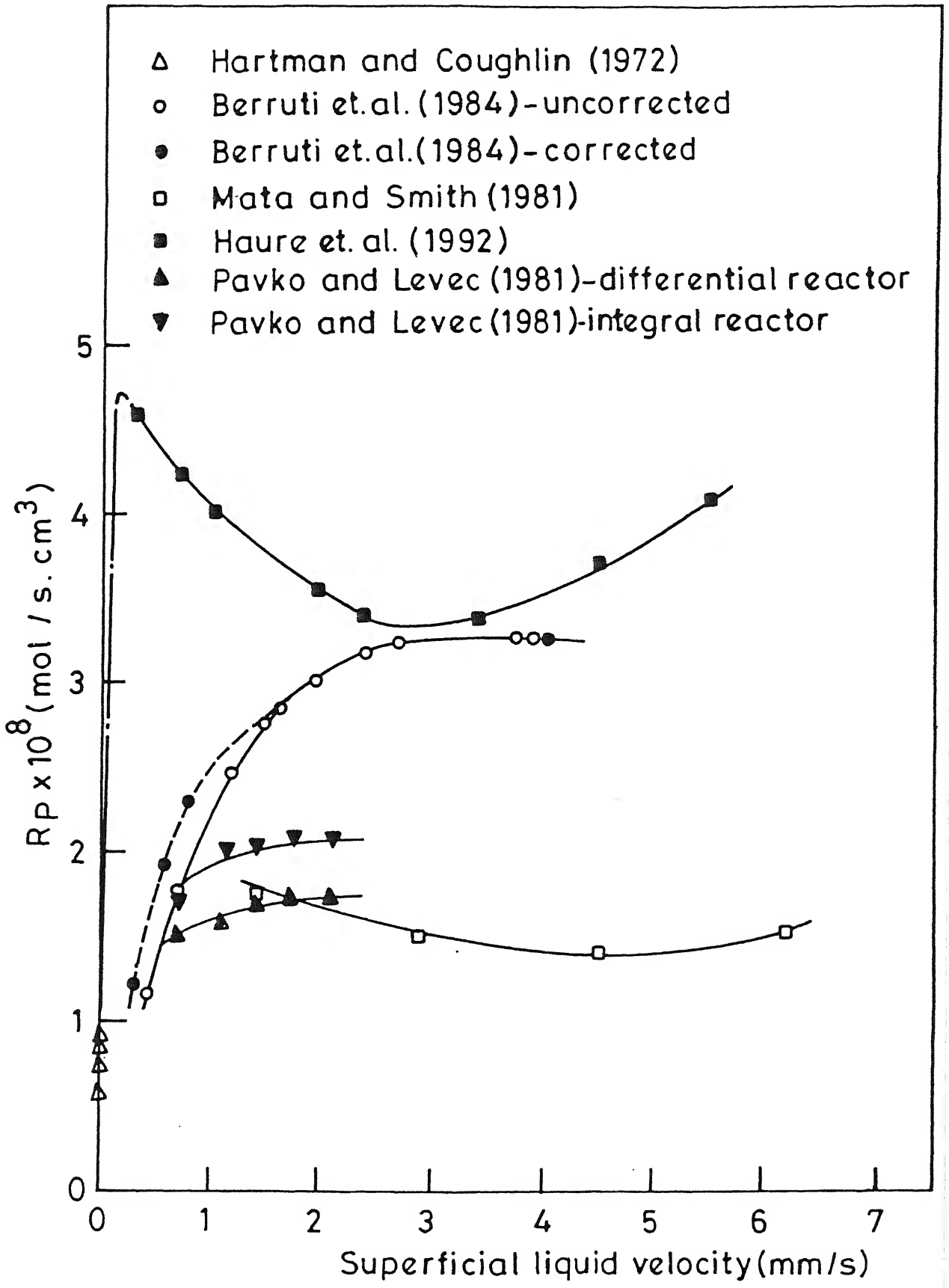

Fig.2 Oxidation rate of sulfur dioxide with superficial liquid velocity.

Mata and Smith (1981) attribute the minimum to the interaction between two conflicting effects. At high liquid flow rates, flowing liquid covers most of the outer surface of the catalyst particles. A decrease in the liquid flow reduces the mass transfer rate between gas and particle because of reduced turbulence in the liquid. Hence the global rate decreases. But, as the liquid flow rate is reduced further, rivulet flow develops and regions are created on the catalyst particles that are "gas-covered" (Herskowitz and Smith, 1978) or "gas-exposed". Since a liquid film is no longer present at the gas-exposed sites, the rate of mass transfer is high. Eventually, the increase in gas-exposed surface more than offsets the reduction in liquid turbulence. At this point the global rate of reaction increases as the liquid flow rate decreases. Haure et al. (1992) attempted to investigate the source of this unexpected behavior. He observed that at low liquid flow rates, steady state is attained remarkably slowly, requiring upto 5h. During this period, rate continuously increases. He concluded that, from the description of experimental procedures, some investigators assumed steady state to exist after a set time interval regardless of flow rate which might have caused the conflicting behavior.

1.3 Objective of the present Investigation

A close scrutiny of the literature indicates that adequate attention was not paid to the mode of operation in reaction rate measurements.

In this present study experiments were conducted to observe the reaction rate trends with different startup

procedures viz.,prewetted and non-prewetted beds which are expected to behave differently at the same liquid flow rates. The hydrodynamic studies of Lutran et al. (1991) and also the liquid flow distribution studies conducted in this test reactor with dry and prewetted beds also support the behaviour difference of these modes of operation. Finally, mass transfer coefficients are evaluated assuming complete wetting of catalyst bed in prewetted mode of operation and compared with Goto and Smith's correlations.

CHAPTER 2
LIQUID FLOW DISTRIBUTION STUDIES

2.1 Introduction

Experiments were conducted to observe the effect of startup procedure,viz., prewetted and non-prewetted bed modes on the liquid flow distribution. Liquid flow distribution measurements were made at different liquid velocities in the range of 0.5-3 kg/m^2-s. In this Chapter brief descriptions of the apparatus and procedure used for making these measurements is given. Critical observations made on the effect of startup procedure on liquid flow measurement at different liquid velocity are discussed.

2.2 Experimental

2.2.1 Description of Experimental Setup for Liquid Flow Distribution Studies

A schematic of the trickle-bed is shown in Figure 3. The trickle-bed was designed in such a way that two types of measurements, viz., liquid flow distribution and reaction rate measurements - could be made. The trickle-bed consists of a gas-liquid distributor, a packed bed section (or the test section) and an end section. A liquid collection device was used as the end section for the measurements of liquid flow distribution. A gas-liquid separator was used for reaction rate measurements.

The distributor was provided with 88 stainless steel capillaries of 0.08 cm ID and 7.0 cm length as shown in Fig.3a. The capillaries were fixed to the top rectangular plate (5.5cm x 8cm) in 8 rows of 11 capillaries each separated from each

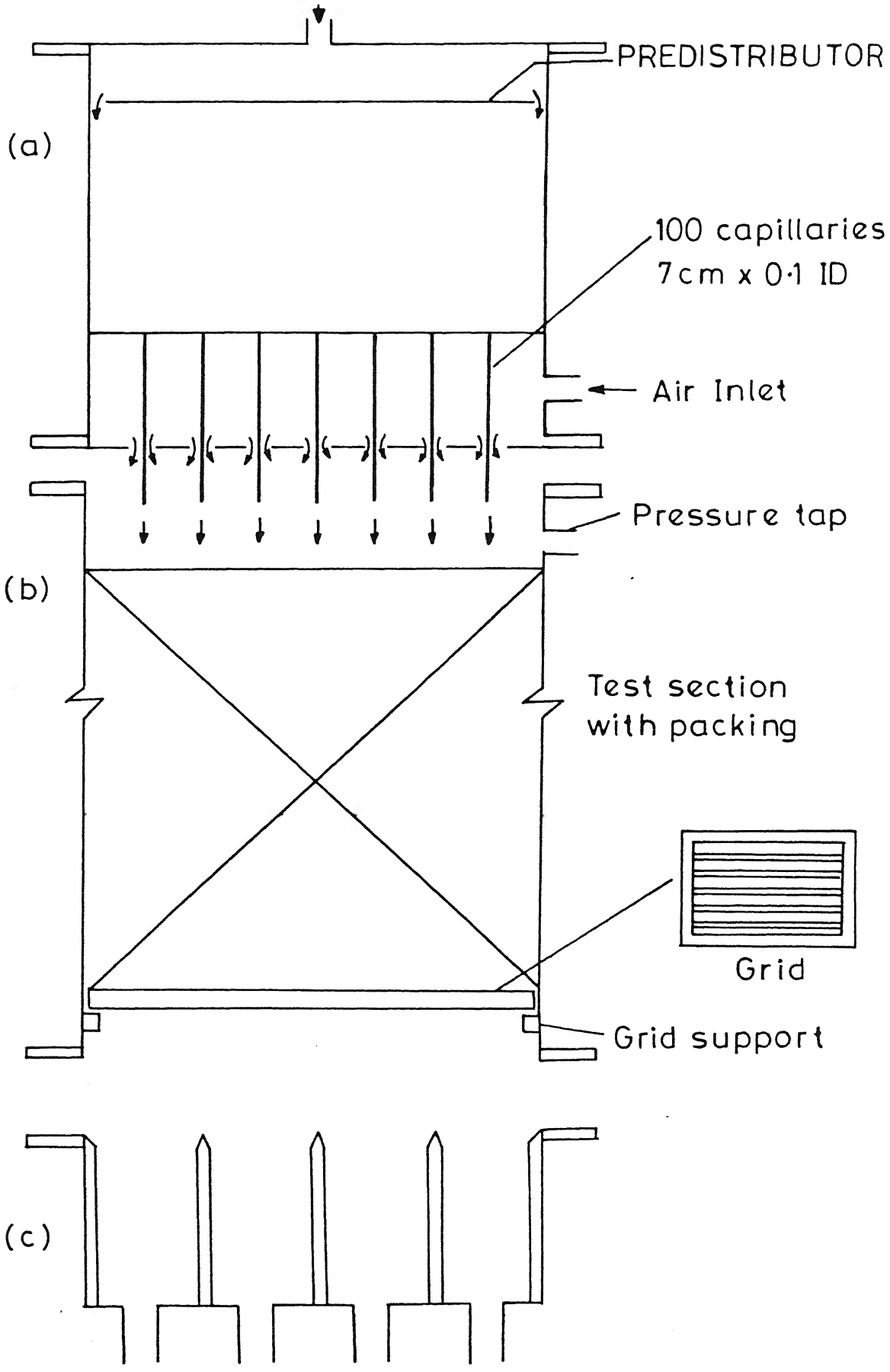
PREDISTRIBUTOR
(a)
100 capillaries
7 cm x 0·1 ID
Air Inlet
Pressure tap
(b)
Test section
with packing
Grid
Grid support
(c)

other or from the wall by 0.6cm. They passed through the circular holes of 0.3cm ID having the same spacing of 0.6cm. These capillaries, aligned in parallel provide a good liquid distribution over the packing. A nozzle was provided in the chamber formed between the two plates to introduce the gas. A horizontal plate was provided just below the liquid inlet as predistributor to direct the liquid flow towards the wall in order to maintain a smooth liquid interface. The liquid entered the packed bed section through the capillaries and the gas through the annular space between the capillaries and circular holes in the bottom plate.

The test section is a plexiglas column having a rectangular cross-section, with inner dimensions of 5.5 x 8cm. The height of the column was 25 cm. Plexiglas sheets were assembled using chloroform to form the rectangular columns of the test section, distributor and the end section.

The collecting device which forms the end section of the trickle-bed reactor consists of 16 equal sized rectangular cells of 5.8 cm height. The upper edge of the cell walls were beveled to a fine line to minimize the influence of the collecting device on the flow distribution. Each cell was provided with a tube through which gas and liquid were discharged.

The equipment used for this liquid distribution measurements is shown in schematic form in Fig.4. Water and air were employed as liquid and gas phases respectively.

Air from a compressor is led through the surge tank, at a controlled flow rate through a gas rotameter to the gas inlet of

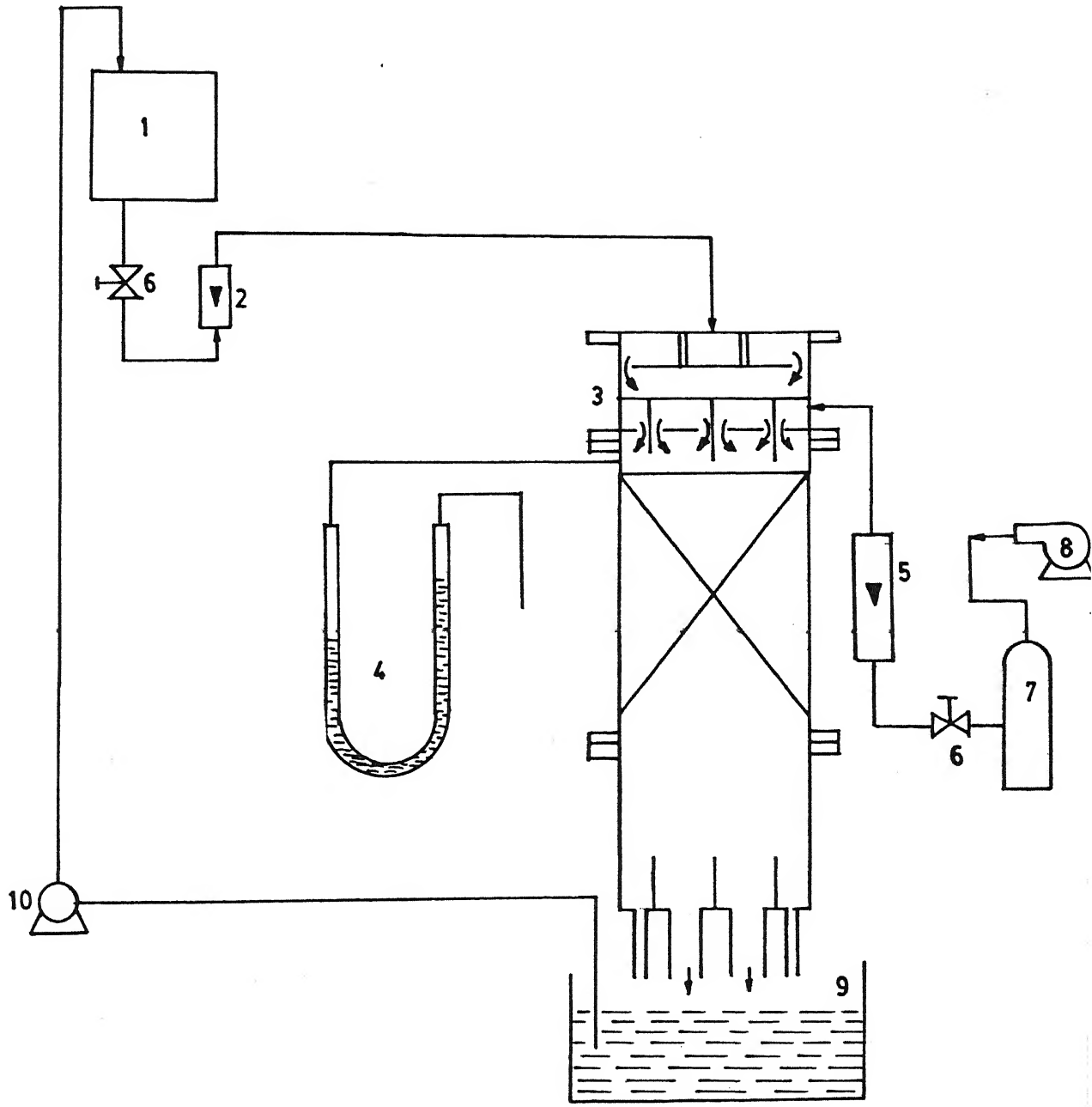

1. Demineralized water tank
2. Liquid rotameter 3. Trickle-bed reactor
4. Manometer for pressure drop measurement
5. Gas rotameter 6. Flow regulator (Needle valve)
7. Air surge tank 8. Air compressor
9. Water tub 10. Water lifting pump

Fig. 4 Schematic diagram of the apparatus used for liquid flow distribution measurements.

the trickle-bed reactor (TBR). Demineralized water from a water tank enters the liquid inlet of the TBR via a rotameter. A manometer connected across the TBR measures the pressure drop in the column.

2.2.2 Experimental Procedure:

Experiments were conducted with two different startup procedures, with non-prewetted and prewetted beds respectively at the start of a run. In the non-prewetted bed mode, the liquid was introduced at a desired flow rate over a bed of dry particles. Subsequently the flow of gas was initiated. In prewetted bed mode, the liquid flow was set at a desired value. Then the bed was flooded with liquid by closing the outlets. Once the liquid level reaches the top of the packing, the outlets were opened to drain the excess liquid while maintaining the liquid flow. Then the gas flow rate was set to a desired value.

2.3 Flow Distribution Measurements

The liquid collection device and the packed bed section were packed with the particles. The continuity of the bed into the cells minimize the cell effect on flow distribution. The flow rates at the 16 outlets of the liquid collection device were measured at regular intervals until steady state was reached. Once the steady state had been attained, the percent liquid flow distribution was calculated by dividing the flow rates at each cell with the total liquid flow rate. The pressure drop across the bed was measured using a manometer.

2.4 Results and Discussions

2.4.1 Non Prewetted Beds

Liquid flow distribution was obtained in non-prewetted mode of operation with BPL type granular activated carbon (supplied by Calgon Carbon Corporation, Pittsburgh, USA) of 12-30 mesh size (equivalent diameter - 0.94 mm). The details of the physical properties are given in Table 2.1. The liquid flow distribution measurements were made at different liquid mass velocities in the range of 0.5 - 3 kg/m^2-sec at a fixed gas mass velocity of 0.01 kg/m^2-sec. The operating conditions for these measurements are summarized in Table 2.2.

Fig. 5a and 5b depicts the liquid flow distribution at a liquid velocity of 0.5 kg/m^2-sec at a fixed gas velocity of 0.01 kg/m^2-sec in non-prewetted mode of operation at different times with porous granular activated carbon particles. It is observed that cells 1,2 and 5 have not received the liquid from the start of the run until the steady state is reached, suggesting that 20% of the bed is not receiving liquid. It should be noted that the cells 1,2 and 5 are all near the wall of the liquid collection device. At liquid flow rates as low as 0.5 kg/m^2-sec and in non-prewetted mode of operation, most of the liquid might be flowing in the form of tortuous filaments. A filament is a stream of liquid flowing down the bed. It can be considered to be a string of liquid pockets and a liquid pocket fills the inter particle pore space formed by more than two particles. These filaments once formed at the start of the run persist till the attainment of steady state since there is not enough liquid flow

Table 2.1

Physical Properties of Type BPL Granular Activated Carbon

Size	12-30 mesh
Mean diameter, mm	0.94
Total surface area (N_2, BET method), (m^2/g)	1050-1150
Apparent density (bulk density), (g/cm^3)	0.48
Particle density, g/cm^3	0.80
Particle porosity	0.6
True solid-phase density, g/cm^3	2.1
Pore volume, cm^3/gm	0.8

Table 2.2

Operating Conditions for liquid flow distribution measurements

Temperature	$25^{o}C$
Pressure	1 atm.
Liquid phase	Deionized water
Liquid mass velocity	0.5-3 kg/m^2-s
Gas phase	Atmospheric air
Gas mass velocity	0.01 kg/m^2-s
Solid phase	Granular activated carbon
Particle size (d_p)	0.94 mm
Bed Height	19 cm
Bed Porosity	0.27

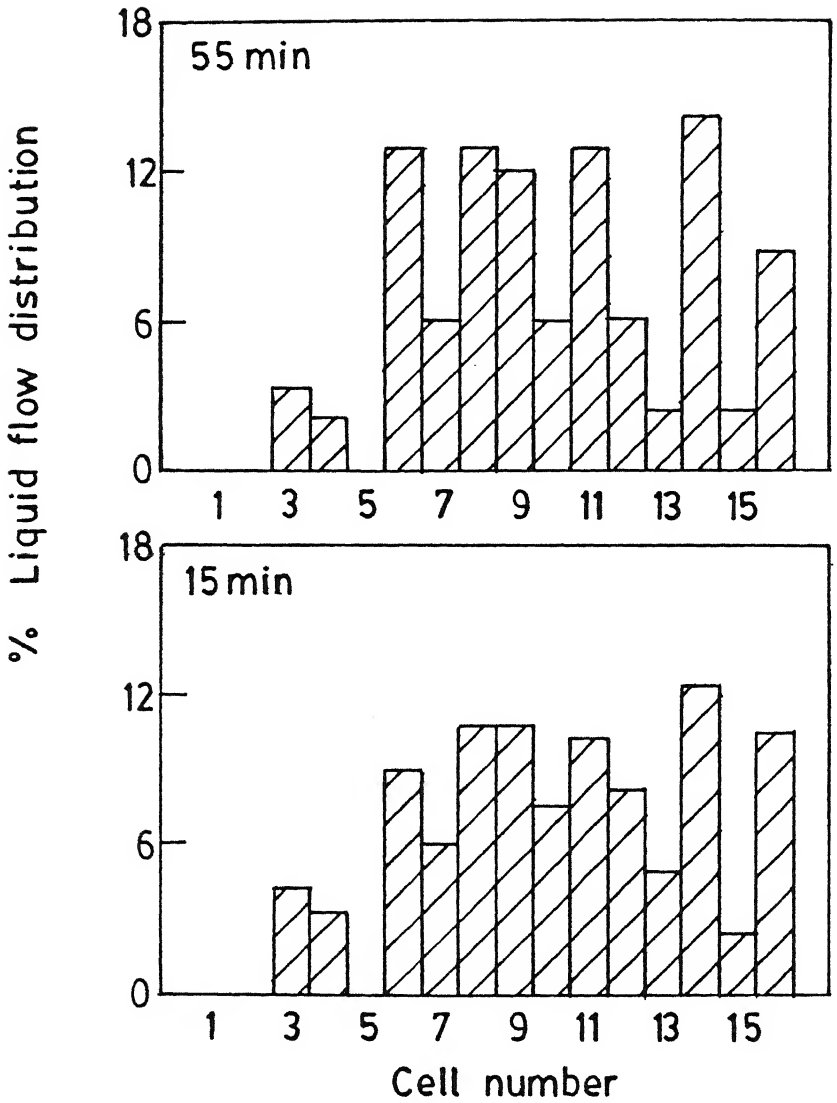

Fig.5a Percent liquid flow distribution versus the cell number at different times in a non-prewetted bed.
Operating Conditions: 0.94 mm granular activated carbon particles, liquid mass velocity = 0.5 kg/m^2-s, gas mass velocity = 0.01 kg/m^2-s.

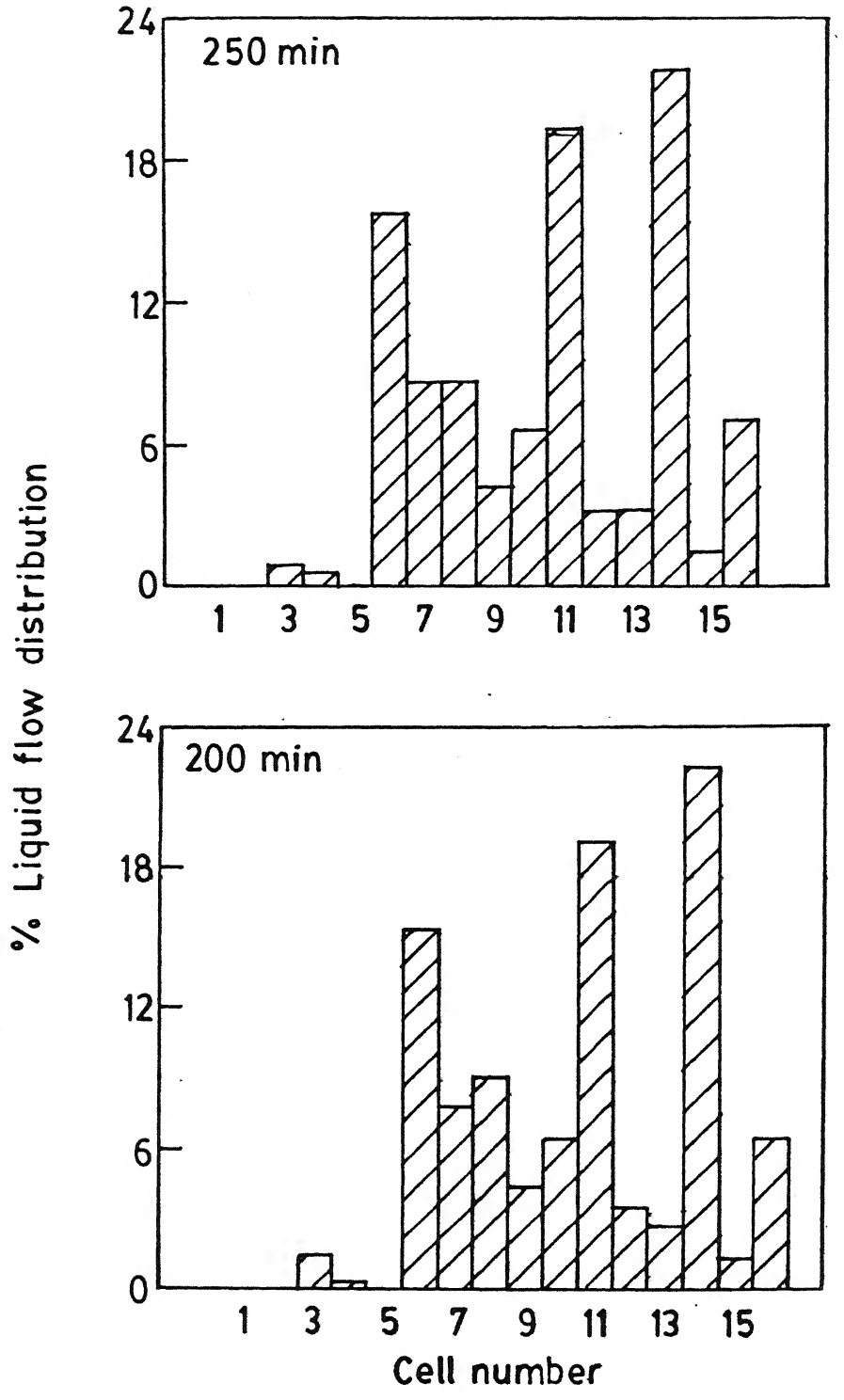
250 min
200 min
% Liquid flow distribution
Cell number
0
6
12
18
24
1
3
5
7
9
11
13
15

FIG. 5 b

(low liquid flow rate) for the expansion of these filaments, leaving approximately 20% of the bed being occupied by dry zones. This is also reflected in the pressure drop measurements. The pressure drop varied in the initial period and was more or less constant at 0.9 cm within 15 min. from the start of the run. Here the flow attained steady state in about 2 h. Hence it could be inferred that the gas and liquid were not flowing uniformly thought the bed cross-section and there are zones in the bed where only gas is flowing and the zones were both liquid and gas are flowing. However, a situation could occur in which a cell is receiving liquid because of liquid flow only or because of the bed being partly occupied with a dry zone and the rest with a liquid zone. The latter phenomenon can occur at the interface of a filament and a dry zone which will give rise to gas-liquid flow through the cell. Therefore, the flow texture at any cross-section of the bed could be a combination of dry zones, gas-liquid flow zones, filament flow zones.

By using computer aided tomography (CAT) Lutran et al. (1991) also observed the filament flow at low liquid flow rates in a trickle-bed reactor with a quiescent gaseous phase when operated in dry mode.

Lazzaroni et al. (1989) have reported that the pressure drop attained steady state in 15 min. for the trickle-bed packed with alumina particles of 2.9 mm using a single liquid inlet.

It is interesting to note the change in liquid flow distribution after 55 mins., at which time slowly the cells, 3,4,9,12 and 13 started receiving less fluid and the cells 6,11

and 14 started receiving more fluid. Finally at steady state, there was marked increase in the flow rates through the cells 6,11 and 14 and appreciable decrease in the flow through cells 3,4,9,12 and 13. The flow appears more uniform at 55 min. than at 200 mins. as can be seen from the figure 5.

A possible reason for this for the density for more non uniform flow to prevail at steady state could be the configuration , orientation and wettability of the catalyst particles, in the region of the bed, where there is filament flow, and the surface tensional forces depending on which the position and shape of the filament must have changed to a convenient one causing changes in the flow through cells as mentioned above. Hence, it appears that these filaments take different tortuous shapes depending on the orientation or configuration of the catalyst particles in these regions of the bed. From this observation it can be concluded that in the case of dry mode of operation, the flow is more non-uniform at steady state occuring to the existence of dry zones, and the filament flow rather than film flow, as 20% of the bed is still dry through which the gas finds a less resistant path. At low liquid flow rates the filaments once formed, tend to stabilize themselves rather than extend throughout the bed due to surface tensional forces.

At slightly high liquid flow rate of 1 kg/m^2-sec, the liquid flow distribution with non-prewetted mode of operation at different times with the same catalyst particles is shown in figures 6a and 6b. It is observed that the cells 1,2 and 13 were not at all receiving the liquid from the start of the run (till 55

min). However, as the time progressed they received a small fraction of the liquid of about 0.2% through cells 1 and 2 and about 0.7% through cell 13. Even in this case of slightly increased flow rate the bed still had dry zones. This suggests that under these conditions only a few new filaments were formed and to accommodate the increased liquid flow rate there is a slight lateral expansion of the filaments as the flow attains steady state as can be seen from the liquid flow distribution histogram in Fig 6. It is interesting to note from this figure that the liquid flow distribution is relatively more non-uniform at 55min and there is slight gradual change to a more uniform distribution towards the steady state. This is in contrast to the observation made at 0.5 kg/m^2-sec liquid mass flow rate, where the gas changes from relatively uniform flow to a non-uniform one. A possible explanation is that the increased liquid flow causes slight expansion of the filaments and moreover for the same reasons as those of the flow distribution at 0.5 kg/m^2-sec liquid flow rate, the movement of the filaments to more stable positions and shapes depending on the configuration and orientation of the particles could have caused these changes in the flow distribution either from uniform to non-uniform flow or from non-uniform to uniform flow as it might appears from the histogram. Even in this case the pressure drop attained a steady value of 2.6 cm of water within 15 minutes from the start of the run. The pressure drop is higher than the value at lower liquid flow rate as expected. Since the bed is still dry through which the gas can escape the pressure drop attained steady value faster (in < 15 min). This

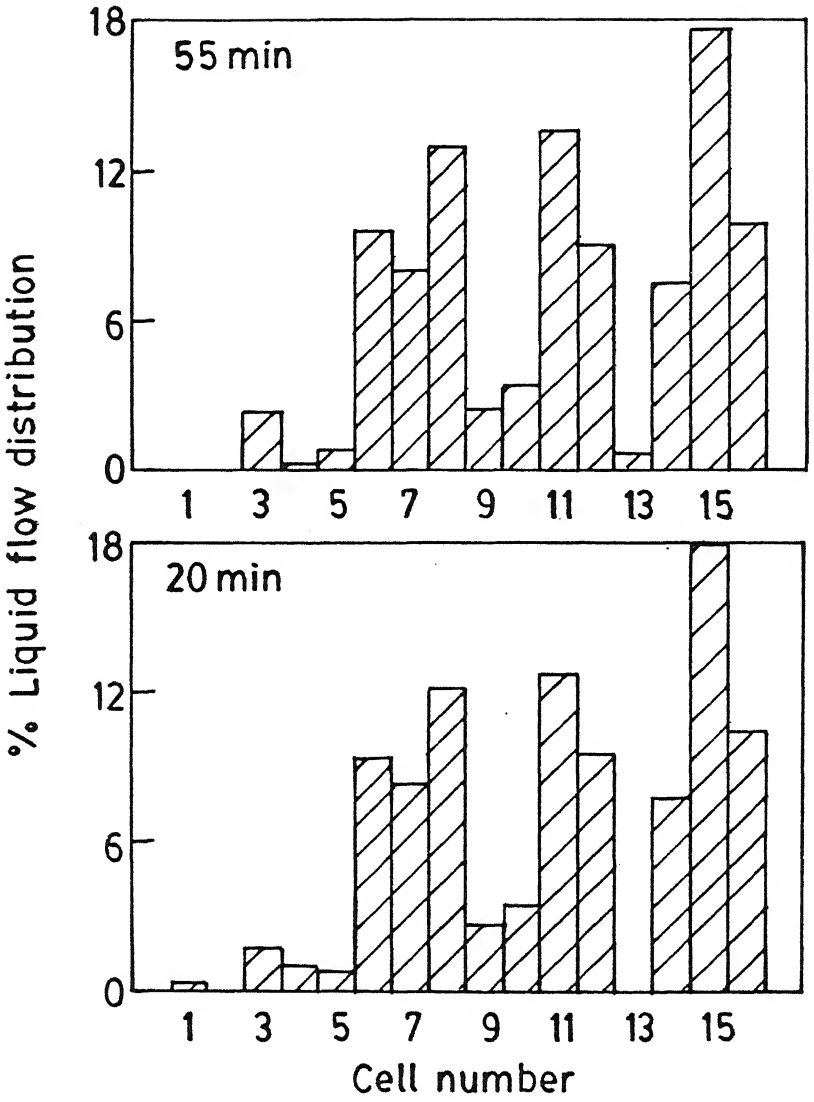

Fig.6a Percent liquid flow distribution versus the cell number at different times in a non-prewetted bed.
Operating Conditions: 0.94 mm granular activated carbon particles, liquid mass velocity = 1.0 kg/m^2-s, gas mass velocity = 0.01 kg/m^2-s.

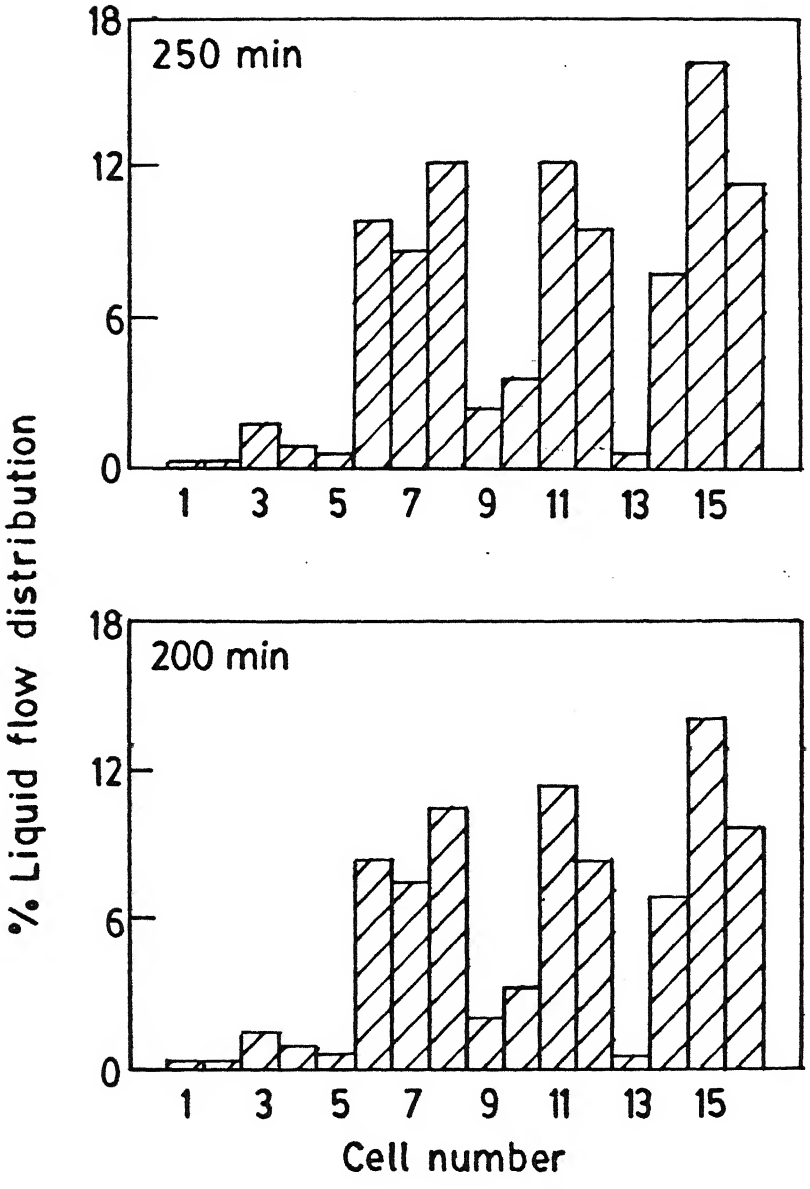
250 min
200 min
18
12
6
0
1 3 5 7 9 11 13 15
% Liquid flow distribution
Cell number

FIG. 6b

fact also confirms the movement of the filaments rather than their expansion leaving dry zone in the packed bed.

2.4.2 Prewetted Beds

The liquid flow distribution in beds packed with the same granular activated carbon particles of equivalent diameter 0.94 mm was studied. The observed flow distribution at 0.5 kg/m^2-sec liquid mass flow rate and at the gas mass flow rate of 0.01 kg/m^2-sec is shown in Fig.7a and 7b at different times. It can be noted from the histogram that the cell 1 was not receiving liquid till 30 min, from the start of the run. However, as the time progressed, it started receiving liquid after 30 min and the steady state was reached in 1hr. It should be noted that even in prewetted mode of operation at very low flow rates as this, the time taken to attain steady state is high. At steady state all the cells are receiving liquid, except the cells 10 and 12. The flow through rest of the cells is more or less uniform. It can be inferred from this observation that the flow through the bed is predominantly film flow in prewetted mode of operation even at as low liquid flow rate as 0.5 kg/m^2-sec. The fact that cell 12 is still receiving high liquid suggests the existence of filament flow in the small fraction of the bed over this cell. Hence, it can be concluded that in case of prewetted bed liquid flows throughout the bed predominantly as thin films over the catalyst particles even at low liquid flow rates and the flow distribution, however, is non-uniform.

The liquid flow distribution at high mass liquid flow rate of 1 kg/m^2-sec at the same gas velocity of 0.01 kg/m^2-sec with the

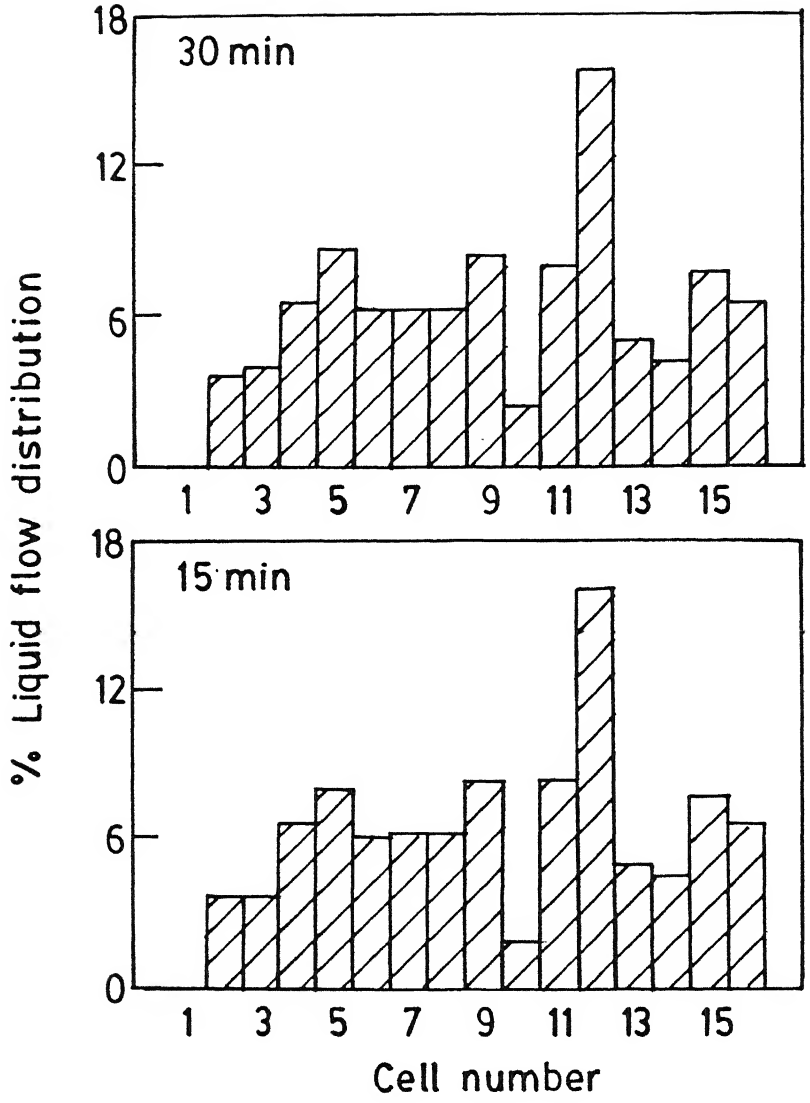

Fig.7a Percent liquid flow distribution versus the cell number at different times in a prewetted bed.
Operating Conditions: 0.94 mm granular activated carbon particles, liquid mass velocity = 1.0 kg/m^2-s, gas mass velocity = 0.01 kg/m^2-s.

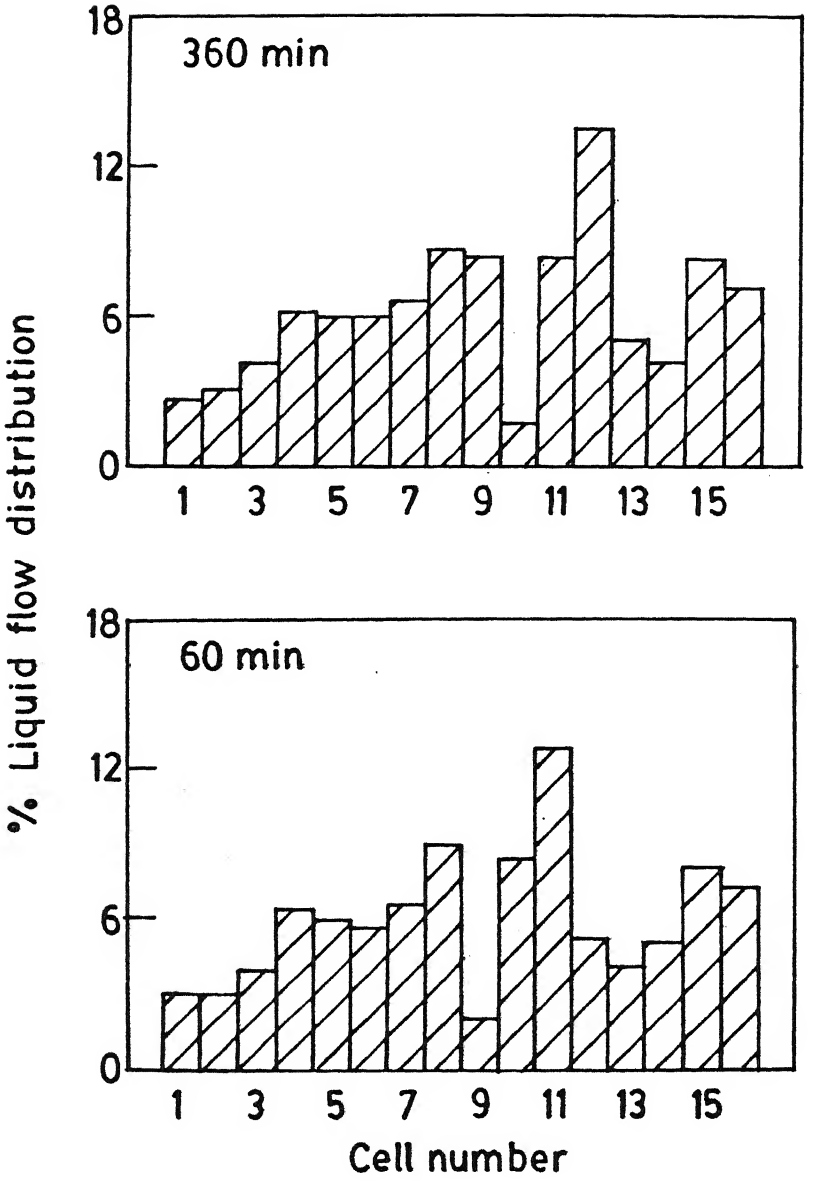
360 min
60 min
% Liquid flow distribution
Cell number
18
12
6
0
1
3
5
7
9
11
13
15

FIG. 7b

same packing, at different times is shown in Fig 8a and 8b. It can be noted from this figure that the flow attained steady state within 15 minutes of operation. It is also evident that the liquid distribution is not uniform across the bed. The liquid flow distribution is deviating by a maximum of ± 50% of the mean value. However, compared to non-prewetted beds and prewetted beds at very low liquid flow rates, the liquid flow distribution is more uniform in this case of prewetted mode of operation. This is expected since prewetting of the bed results in the formation of pendular structures (rings and bridges) connected with a thin film of liquid over the particles. This increases the interconnnectivity between particles and leads to improved liquid flow distribution.

The above observations reveal that the liquid flow distribution depends upon the mode of operation (non-prewetted or prewetted) of the bed. Since the liquid flow distribution is expected to influence the rate of reaction, the mode in which the bed was operated needs to be mentioned in the reporting the reaction rate measurements. The effect of mode of operation on the reaction rate is discussed in the next chapter.

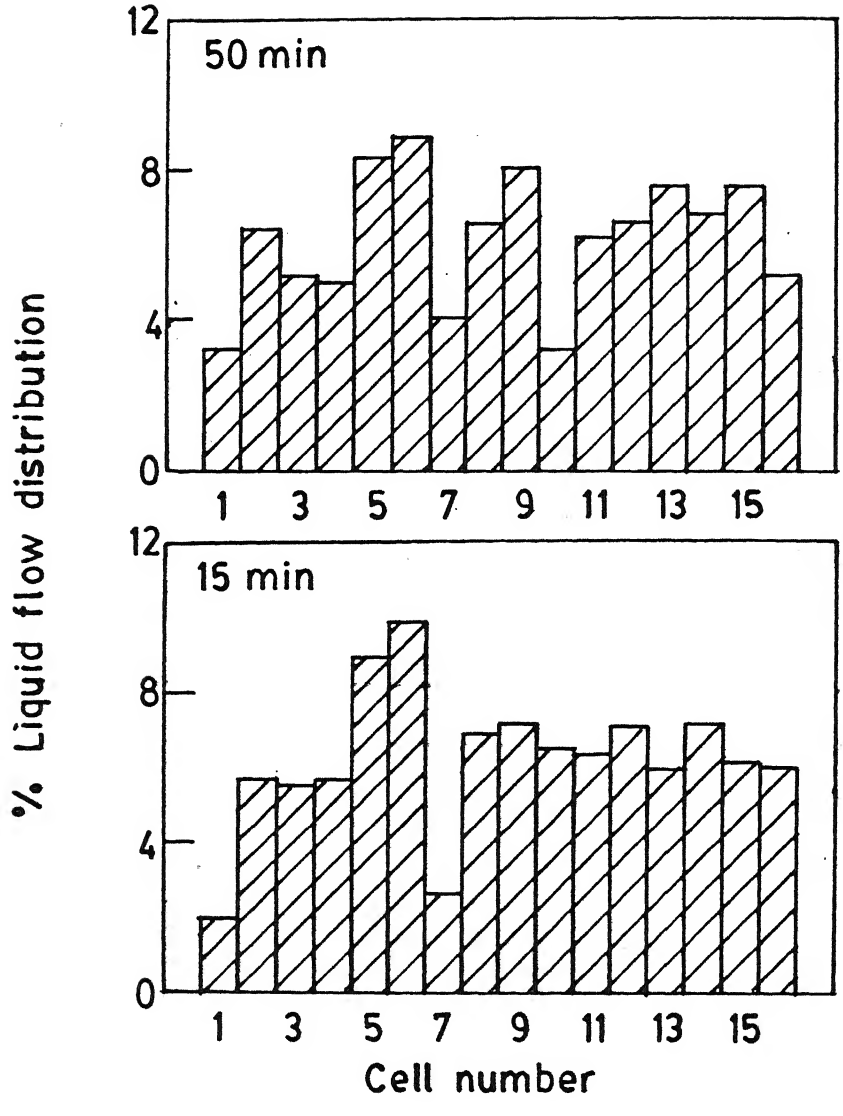

Fig. 8a Percent liquid flow distribution versus the cell number at different times in a prewetted bed.
Operating Conditions: 0.94 mm granular activated carbon particles, liquid mass velocity = 1.0 kg/m^2-s, gas mass velocity = 0.01 kg/m^2-s.

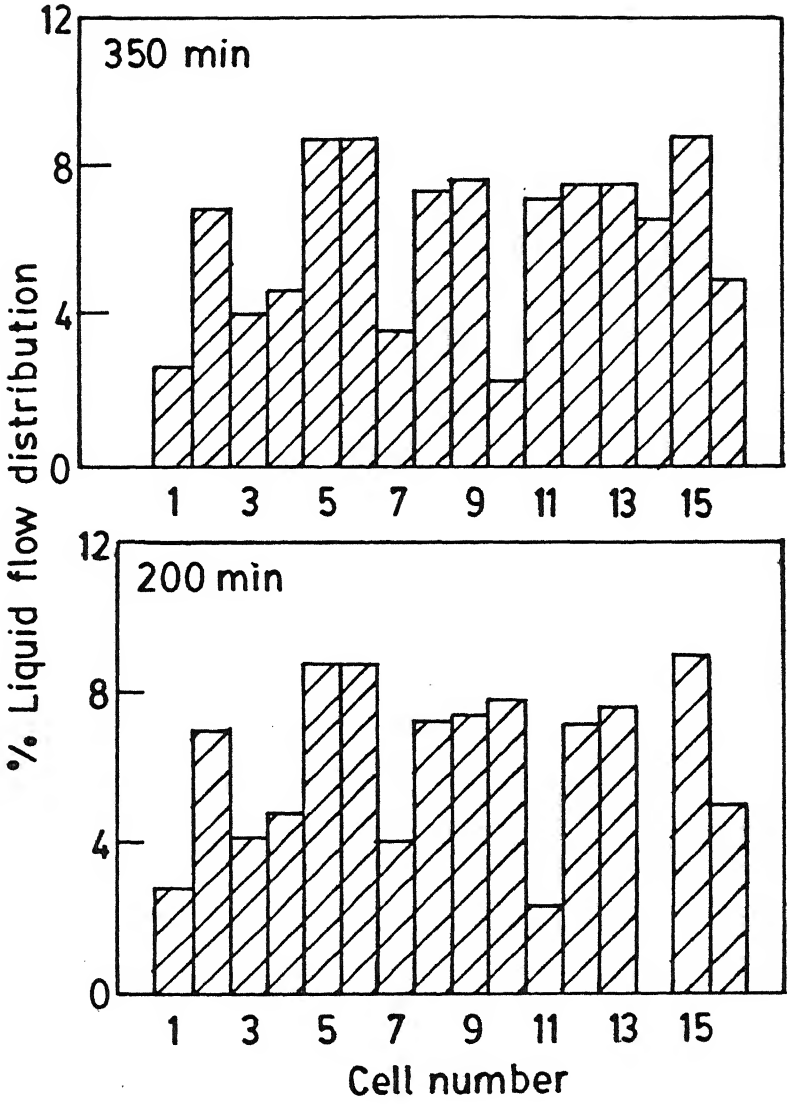
350 min
200 min
% Liquid flow distribution
Cell number
12
8
4
0
1
3
5
7
9
11
13
15

FIG. 8b

CHAPTER 3

REACTION RATE STUDIES

3.1 Introduction:

It was shown that the mode of operation of the bed has significant effect on the liquid flow distribution in a trickle-bed reactor. The reaction rate is expected to depend on the liquid flow distribution and hence on the mode of operation. The effect of startup procedure on the reaction rates has been experimentally studied using the oxidation of SO_2 on activated carbon catalyst as a model reaction. The results of these studies are presented in this chapter. An attempt has been made to propose a plausible model to interpret the experimental data in the prewetted bed.

3.2 Materials

3.2.1 Gases used

The gases used for the SO_2 oxidation study are as follows:

Sulfur dioxide (SO_2): Liquid sulfur dioxide was supplied by Medical Engineers India (Pvt) Limited, Delhi.

Oxygen (O_2): Atmospheric air was used as the source of oxygen.

3.2.2 Materials used for the chemical (titrimetric) analysis.

The reagents used for the titrimetric analysis of the effluent liquid sample from the trickle-bed reactor are as follows:

Potassium Iodide (KI): It had a reported minimum purity of 99% and was supplied by New India Chemical Enterprises, Kochi.

Potassium Iodate (KIO_3): It had a reported minimum purity of 98% and was supplied by S.D. Fine - Chem - Ltd., Bombay.

Starch: Extra pure soluble starch was supplied by Merck (India) Ltd., Bombay.

Potassium Hydrogen Pthalate ($KHC_8H_8O_4$): It had a reported minimum purity of 99.95% and was ~~used~~ supplied by S.D. Fine Chem. Ltd., Bombay.

Iodine (I_2): It had a purity of 99.5% and was supplied by New India Chemical Enterprises, Kochi.

Sodium thiosulphate ($Na_2S_2O_35H_2O$): It had a reported purity of 99% and was supplied by New India Chemical Enterprises, Kochi.

Hydrogen Peroxide (H_2O_2): It had a concentration of 99.75% and was supplied by E. Merck (India) Ltd, Bombay.

Sodium hydroxide (NaOH): It had a reported minimum purity of 97% and was supplied by New India Chemical Enterprises, Kochi.

Hydrochloric acid (HCl): The acid had a reported purity of 99.65% and was supplied by E. Merck (India) Ltd., Bombay.

Sulfuric acid (H_2SO_4): The acid had a reported purity of 99% and was supplied by E. Merck (India) Ltd., Bombay.

Phenolphthalein: Phenolphthalein indicator was supplied by S.D's pure - Chem Ltd., Boisar.

3.2.3 Catalyst used for SO_2 Oxidation

The catalyst used for the oxidation of SO_2 in the trickle-bed reactor was supplied by Calgon Carbon Corporation, Pittsburgh, U.S.A.

3.3 Experimental

3.3.1 Equipment Description

The trickle-bed reactor used for the reaction rate measurements is schematically same as that shown in Fig.3 except

for the inclusion of a gas-liquid separator in place of liquid collection device.

In order to study the reaction rates for a wide range of liquid flow rate (1-6 kg/m^2-s), a trickle-bed reactor with slightly different dimensions and distributor design from that used in liquid distribution studies was used in this case.

Here the distributor was provided with 100 stainless steel capillaries of 0.1 cm ID and 7.0 cm length. The capillaries were fixed to the top rectangular plate (6cmx8cm) in rows. Each capillary was separated from the others and from the wall by 0.3 cm. They passed through the circular holes of 0.3 cm ID having the same spacing of 0.6 cm. The rest of the design and operation of the liquid distributor is the same as that used for liquid flow distribution measurements studies (Chapter 2).

The test section had a rectangular cross-section with inner dimensions of 6cm x 8cm. The height of the column was 25cm. Two glass plates formed the front and back panels of the column. These plates were fixed to the stainless steel side plates using an epoxy resin. Two supports (grid supports) of 0.5 cm width each were provided at the bottom of the test section on the stainless steel plates.

The grid employed was made of stainless steel and consisted of metal strips fixed on a frame to form a rectangular grid of 5.9x7.9cm size with a spacing of 0.3 cm between the strips. It rested on the supports provided at the bottom of the packed section. Since the particle size used for reaction rate measurements is 0.21 cm. equivalent diameter, a wire mesh is

placed over the grid.

The end section of the trickle-bed reactor in this study consists of a gas-liquid separator for separating effluent gas and liquid.

The equipment used for the reaction rate measurements is shown in schematic form in Fig.9. Water and air-SO_2 mixture were employed as liquid and gaseous phases, respectively.

Air from a compressor is passed via a surge tank, and a gas rotameter, at a controlled flow rate, to the inlet of the mixing chamber. SO_2 gas from the gas cylinder enters the mixing chamber via a soap bubble flow meter. Air and SO_2, after mixing in the mixing chamber, enter the trickle-bed reactor. Demineralized water from a water tank enters the liquid inlet of the trickle-bed reactor via a rotameter. A manometer connected across the reactor measures the pressure drop in the column.

3.3.2 Experimental Procedure

Experiments were conducted with two different startup procedures, with non-prewetted and prewetted beds respectively at the start of a run, with BPL type granular activated carbon (supplied by Calgon Carbon Corporation, Pittsburgh, USA) of 6-16 mesh size (equivalent diameter of 0.21 cm). The details of the physical properties are given in Table 3.1.

In the non-prewetted bed mode the liquid was introduced at a desired flow rate over a bed of dry particles. Subsequently the flow of the air-SO_2 mixture was initiated. In prewetted bed mode, before packing, the carbon particles were soaked in boiling demineralized water for 2h. in order to ensure pore filling as

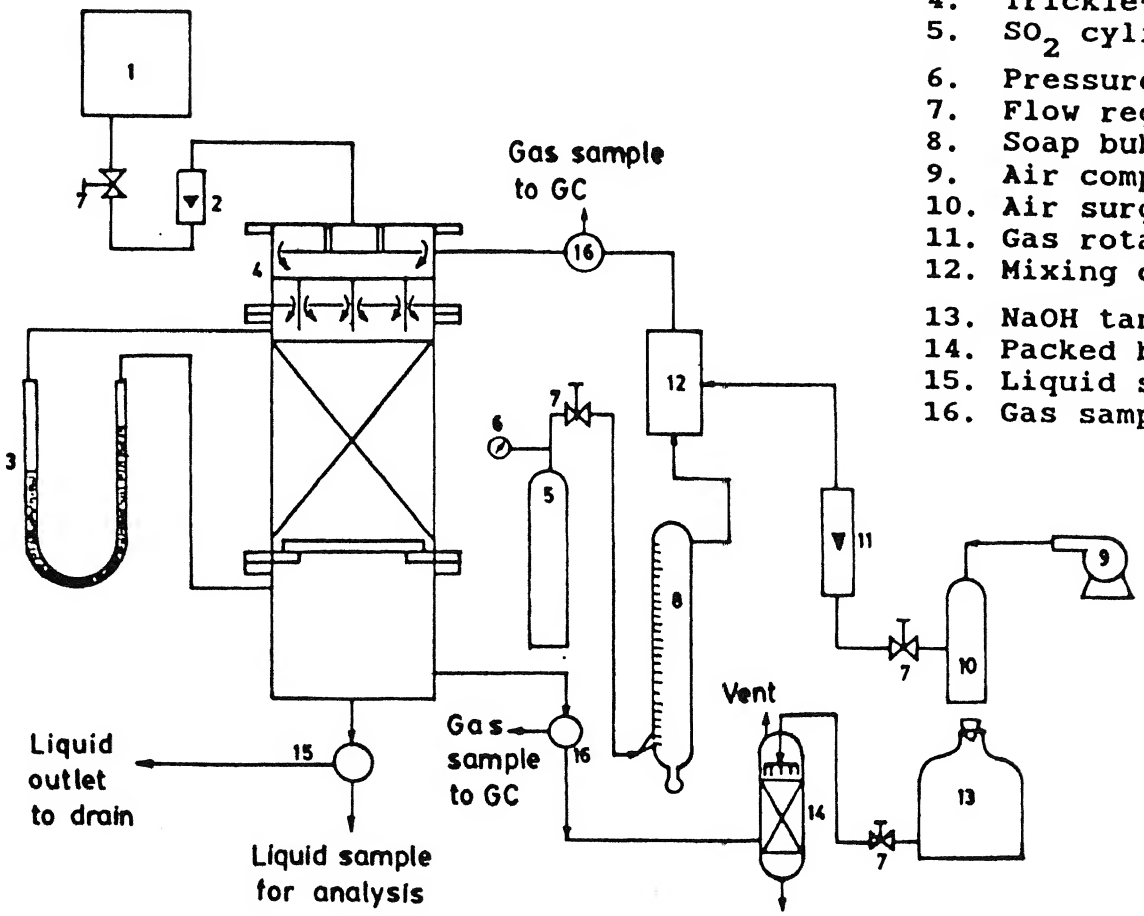

1. Deionized water tank
2. Liquid rotameter
3. Manometer for pressure drop measurement
4. Trickle-bed reactor
5. SO_2 cylinder
6. Pressure regulator
7. Flow regulator (needle valve)
8. Soap bubble flow meter
9. Air compressor
10. Air surge tank
11. Gas rotameter
12. Mixing chamber for air and SO_2
13. NaOH tank
14. Packed bed absorption
15. Liquid sample port
16. Gas sample port

Fig. 9 Schematic diagram of the experimental setup used for reaction rate measurements.

Table 3.1

Physical Properties of Type BPL Granular Activated Carbon

Size	6-16 mesh
Mean diameter,cm	0.21
Total surface area (N_2, BET method), (m^2/g)	1050-1150
Apparent density (bulk density), (g/cm^3)	0.48
Particle density, g/cm^3	0.80
Particle porosity	0.6
True solid-phase density, g/cm^3	2.1
Pore volume, cm^3/gm	0.8

also removing fines. As the bed was packed, the reactor was filled with water; then the particles were added a few layers at a time with compacting and vibrating the reactor tube after each addition. After packing the bed as described, the liquid flow was set at the desired value. Then the bed was flooded with liquid by closing the outlets. Once the liquid reaches the top of the packing, the outlets were opened to drain the excess liquid while maintaining the liquid flow. Then the gas flow rate was adjusted to the desired value.

3.4 Analysis

3.4.1 Analysis of Gas Samples

The gas samples of the inlet and outlet of the trickle-bed reactor were analyzed with a gas chromatograph using thermal conductivity detector (TCD). Porapak-Q to column was used for separating the components. H_2 was used as the carrier gas. A column temperature of $85^{o}C$ was used.

3.4.2 Analysis of Liquid Samples

The liquid effluent sample contains sulfurous acid because of the solubility of SO_2 in water and sulfuric acid as a reaction product.

H_2SO_4 being the reaction product, we are interested in the concentration of H_2SO_4 alone in reaction rate measurements. To get the concentration of H_2SO_4 in a sample containing a mixture of H_2SO_4 and H_2SO_3 , the method suggested by Hartman and Coughlin (1972) was first attempted.

According to the method suggested by Hartman and Coughlin (1972), the concentration of SO_2 in liquid (H_2SO_3) was determined

with 0.1 N iodine solution using a Starch Indicator. In another portion of each sample, dissolved SO_2 was oxidized to H_2SO_4 with H_2O_2 and the combined amount of H_2SO_4 and SO_2 was determined by titration with 0.1 N NaOH solution. The concentration of H_2SO_4 prior to oxidation was obtained as a difference between the combined amount of H_2SO_4 and SO_2 and the amount of SO_2 in the liquid.

Though this method appears perfectly alright, there are certain practical difficulties with it. The hydrogen peroxide which is added to oxidize H_2SO_3 to H_2SO_4 has acidity. This acidity is due to the addition of phosphoric acid to H_2O_2 as a stabilizer when H_2O_2-containing phosphoric acid is added to liquid sample for oxidizing H_2SO_3 to H_2SO_4 and titrated against NaOH, though H_2O_2 is neutral, the phosphoric acid in it reacts with NaOH and can form sodium monophosphate, sodium biphosphate and triphosphate. Also H_2O_2 when added in stoichiometric quantities did not completely oxidize H_2SO_3 to H_2SO_4 at room temperature as noted from control volume experiments. Heating can not be done in these situations as SO_2 might escape. Because of these practical difficulties, this method was not used.

The following method is used in the final analysis of liquid samples.

H_2SO_3 solution is prepared by passing SO_2 through water, and its concentration was determined by Iodimetry. It is mentioned in Modern Inorganic Chemistry by Mellor that SO_2 can be completely expelled on boiling. A sample of H_2SO_3 whose concentration is determined by iodimetry is boiled for 10 min and then cooled.

This then titrated with 0.1 N NaOH solution and its normality was calculated. It is also observed that a small amount of H_2SO_3 is still left in solution after boiling owing to its small solubility which is to some extent detected by NaOH because of the following reactions. H_2SO_3 in water is present as:

$$H_2SO_3 \rightleftharpoons H^+ + HSO_3^-$$

$$HSO_3^- \rightleftharpoons H^+ + SO_3^{2-}$$

$$H_2SO_3 \rightleftharpoons SO_2 + H_2O$$

when treated with NaOH, H_2SO_3 can form.
Na_2SO_3 or $HaHSO_3$: Also Na_2SO_3 formed in water exists in equilibrium as

$$Na_2SO_3 + H_2O \rightleftharpoons NaOH + NaHSO_3$$

Hence a calibration is made on the % of H_2SO_3 detected with NaOH after 10 min. boiling for different concentrations of H_2SO_3 with in the experimental range (Fig.10). Fig.11 shows a plot of H_2SO_3 conc. vs % detected by NaOH after boiling for 10 min. And this data is need to correct the concentrations measured by NaOH as follows.

A sample of liquid leaving the reactor is analyzed for H_2SO_3 concentration. Another sample is boiled for 10 min to expell H_2SO_3 to a large extent (96-98%) and cooled and analyzed with NaOH

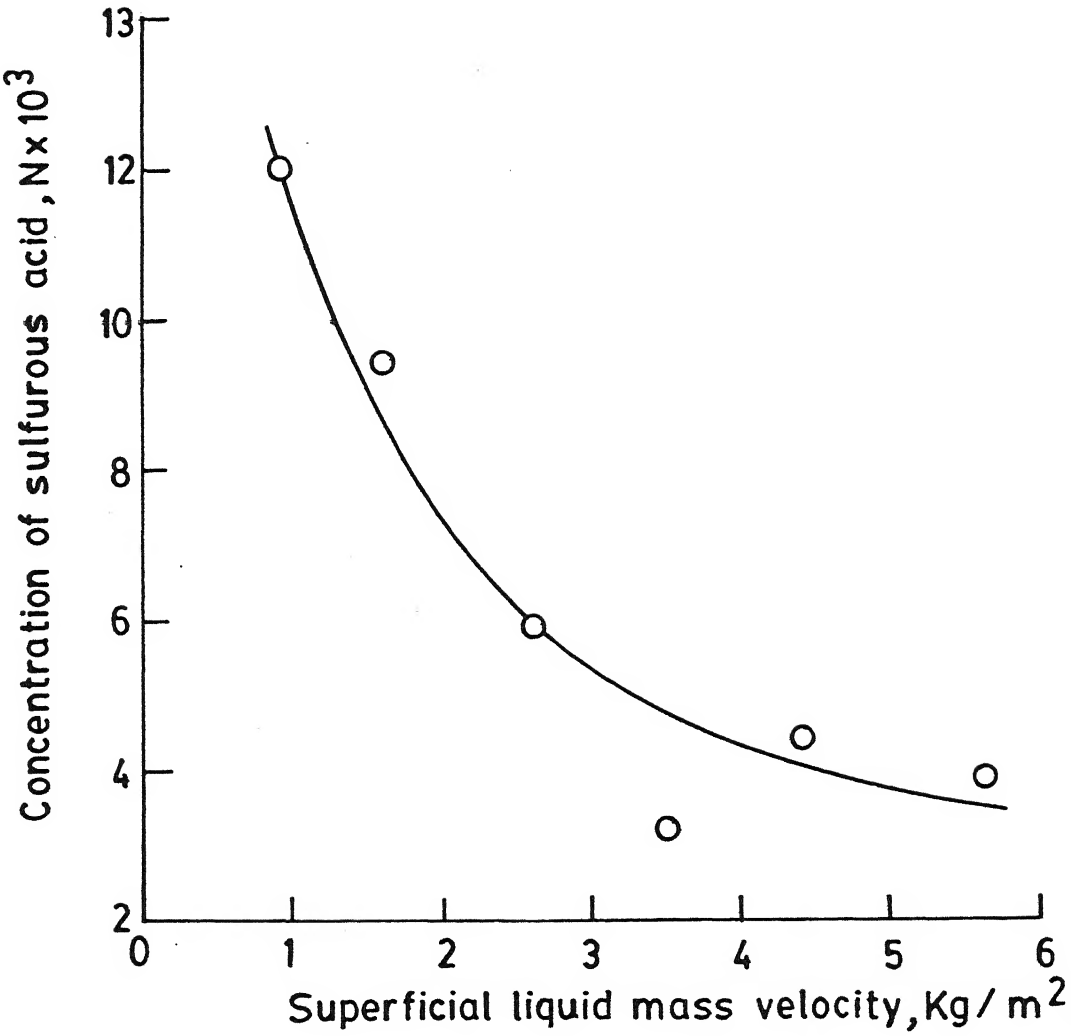

FIG. 10 CONCENTRATION OF SULFUROUS ACID IN THE EFFLUENT LIQUID VS. LIQUID VELOCITY IN A PREWETTED BED

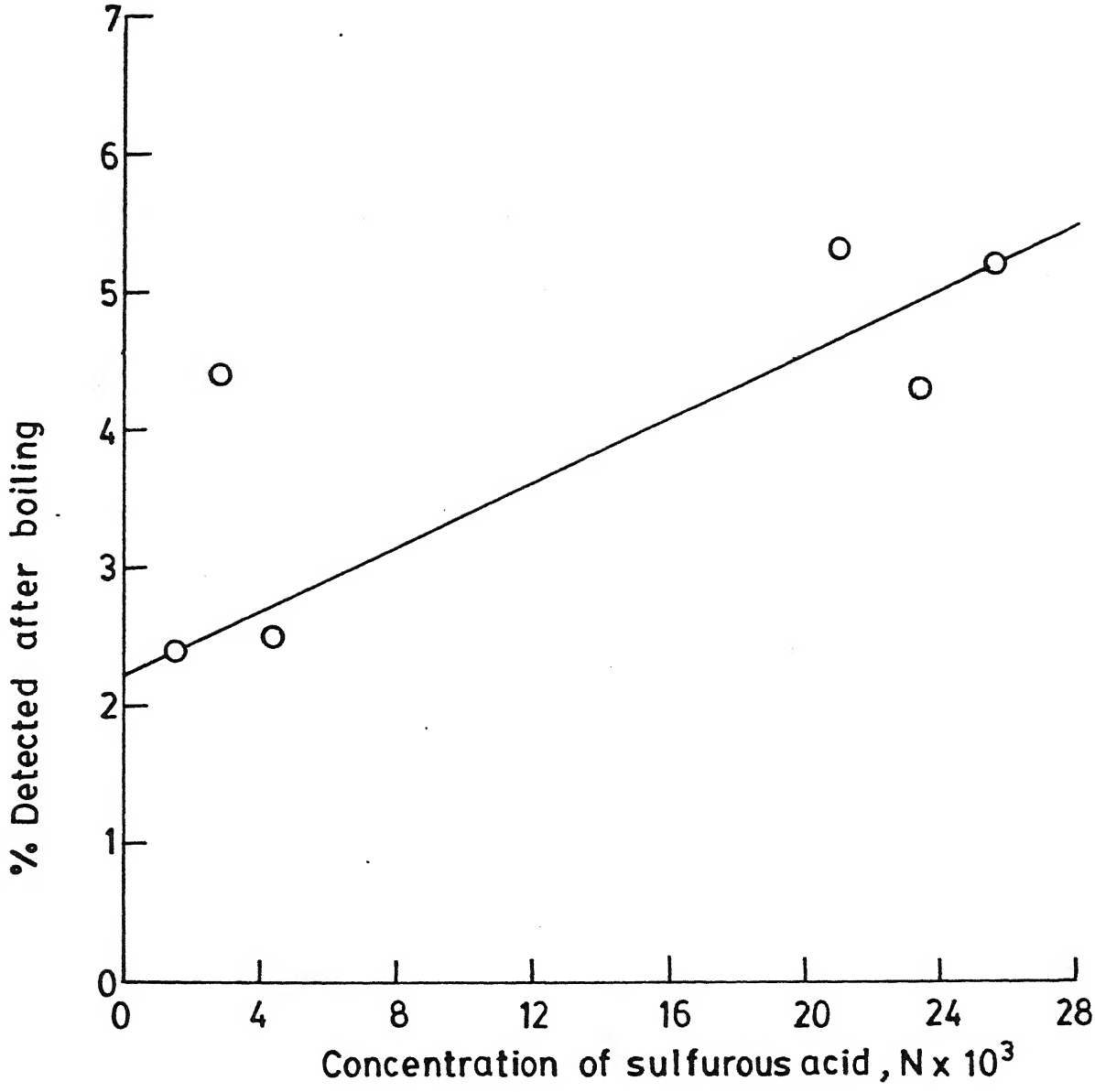

FIG. 11 CORRECTION PLOT FOR SULFUROUS ACID REMAINING AFTER BOILING

solution. The concentration is then corrected for the presence of small amounts of H_2SO_3 after boiling from correction curve (by subtracting from the value obtained from titration with NaOH, the value corresponding to the percentage detected by NaOH after boiling). The concentration obtained after correcting for H_2SO_3 gives the concentration of H_2SO_4 in the liquid sample.

3.5 Results and Discussion

An earlier study of SO_2 oxidation (Hartman and Coughlin (1972)) demonstrated the catalytic activity of activated carbon, for type BPL carbon. The intrinsic rate was found (Komiyama and Smith (1975)) to be zero order with SO_2 and first order with oxygen for gas concentration of 0.3 - 9.0% SO_2 and 5.2 - 21% O_2. The production rate of sulfuric acid reaction ($\bar{R}_{H_2SO_4}$) per unit volume of the empty reactor is calculated from the equation

$$\bar{R}_{H_2SO_4} = \frac{C_{L,H_2SO_4} Q_L}{V_R} = -2 \bar{R}_{O_2}$$

Such average rates were obtained from data for different liquid flow rates at a fixed gas flow rate for both modes of operations. The operating conditions for reaction rate measurements are summarized in Table 3.2.

3.5.1 Prewetted Mode

Fig.12 shows a plot of liquid mass velocity versus reaction rate. The liquid mass velocities were varied in the range of 1-6 kg/m^2-s while maintaining the gas mass flow rate at 0.02 kg/m^2-s with 1.7 volume % of SO_2. Here in this case of prewetted mode of

Table 3.2

Operating Conditions for the reactions rate studies

Temperature	25°C
Pressure	1 atm.
Liquid phase	Deionized water
Liquid mass velocity	1-6 kg/m^2-s
Gas phase	1.7 vol% SO_2; 98.3 vol% Air
Gas mass velocity	0.02 kg/m^2-s
Solid phase	Granular activated carbon
Particle size (d_p)	0.21 cm
Bed Height	20.1 cm
Bed Porosity	0.34

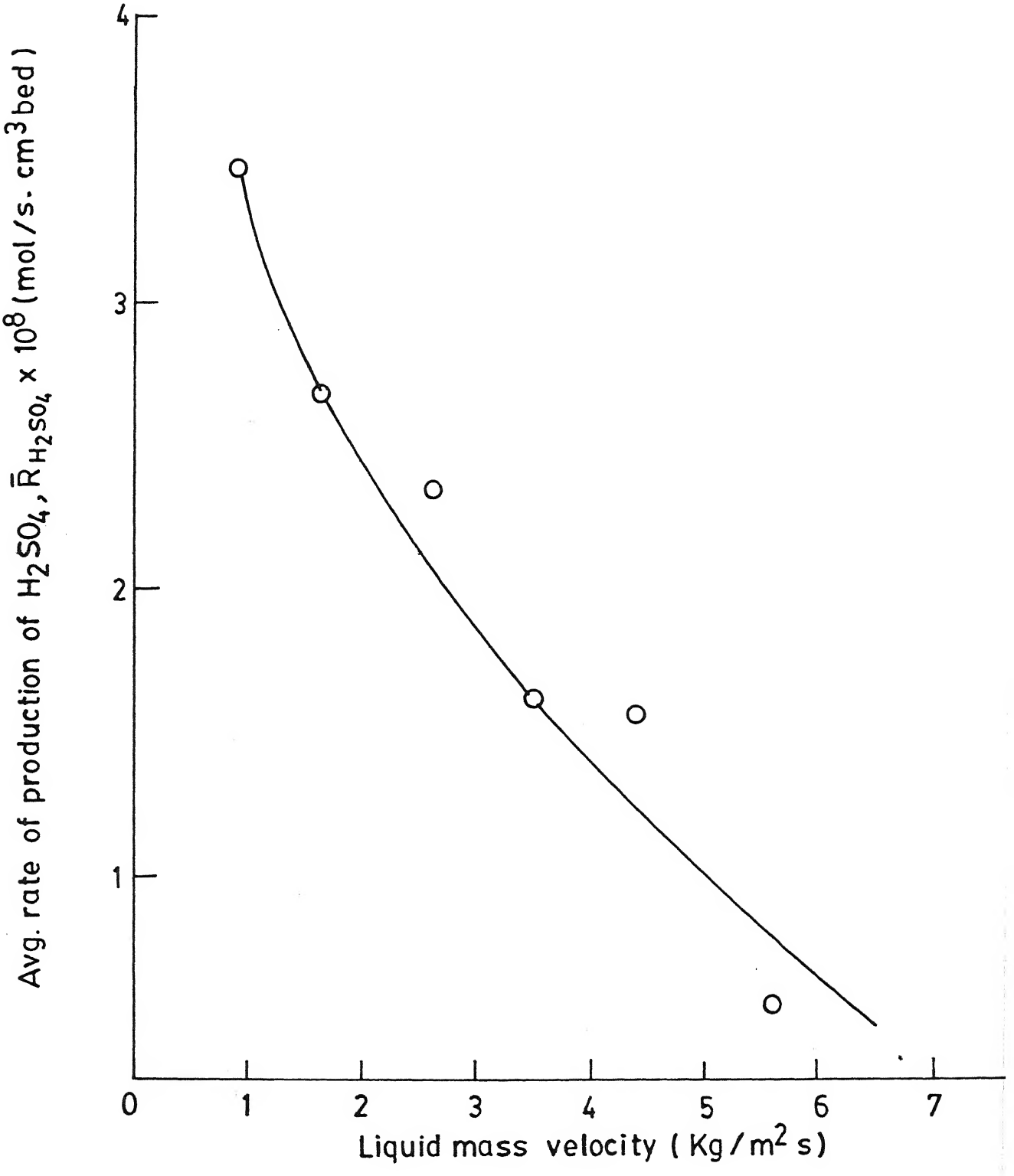

FIG. 12 PRODUCTION RATE OF H_2SO_4 AS A FUNCTION LIQUID VELOCITY IN A PREWETTED BED

operation the rate is observed to decrease with an increase in liquid flow rate. It was noted in the liquid distribution studies that the liquid flows predominantly as thin film over the catalyst particles in prewetted mode of operation. As the liquid flow rate increases, the liquid film thickness over the catalyst particles increases thereby decreasing the rate of transfer of the limiting reactant (oxygen) to the solid-liquid interface, resulting in a decrease of the reaction rate.

3.5.2 Non-Prewetted Mode

In non-prewetted mode of operation the reaction rate measurements were made at different mass liquid flow rates in the range of 1-5 kg/m^2-s at a fixed gas mass velocity of 0.02 kg/m^2-s. The transient behaviour of dry beds at L = 1 and 3 kg/m^2s are shown in Fig. 13 and 14 respectively.

The reaction rate at a liquid velocity of 1 kg/m^2-s in the non-prewetted mode is $2.2 \times 10^{-8} \frac{g\ mole}{(cc\ bed)\ sec}$ whereas in prewetted mode at the same liquid velocity the rate is 3.47×10^{-8}. The rate in case of dry bed decreased by 40% of that in the prewetted bed. The reason for this could be the observed filament flow and dry zones in case of dry mode of operation at low liquid flow rates as observed in liquid distribution measurement. The filament flow through the bed reduces the reaction rates as there is no gas flow through such regions.

The reaction rate at a liquid velocity of 3 kg/m^2-s in dry mode of operation is 2.24×10^{-8} and its value in prewetted case at the same liquid velocity is 2.35×10^{-8}. It is clear from these values of the reaction rates that the rates at this particular liquid flow rate are almost equal in case of non-prewetted and

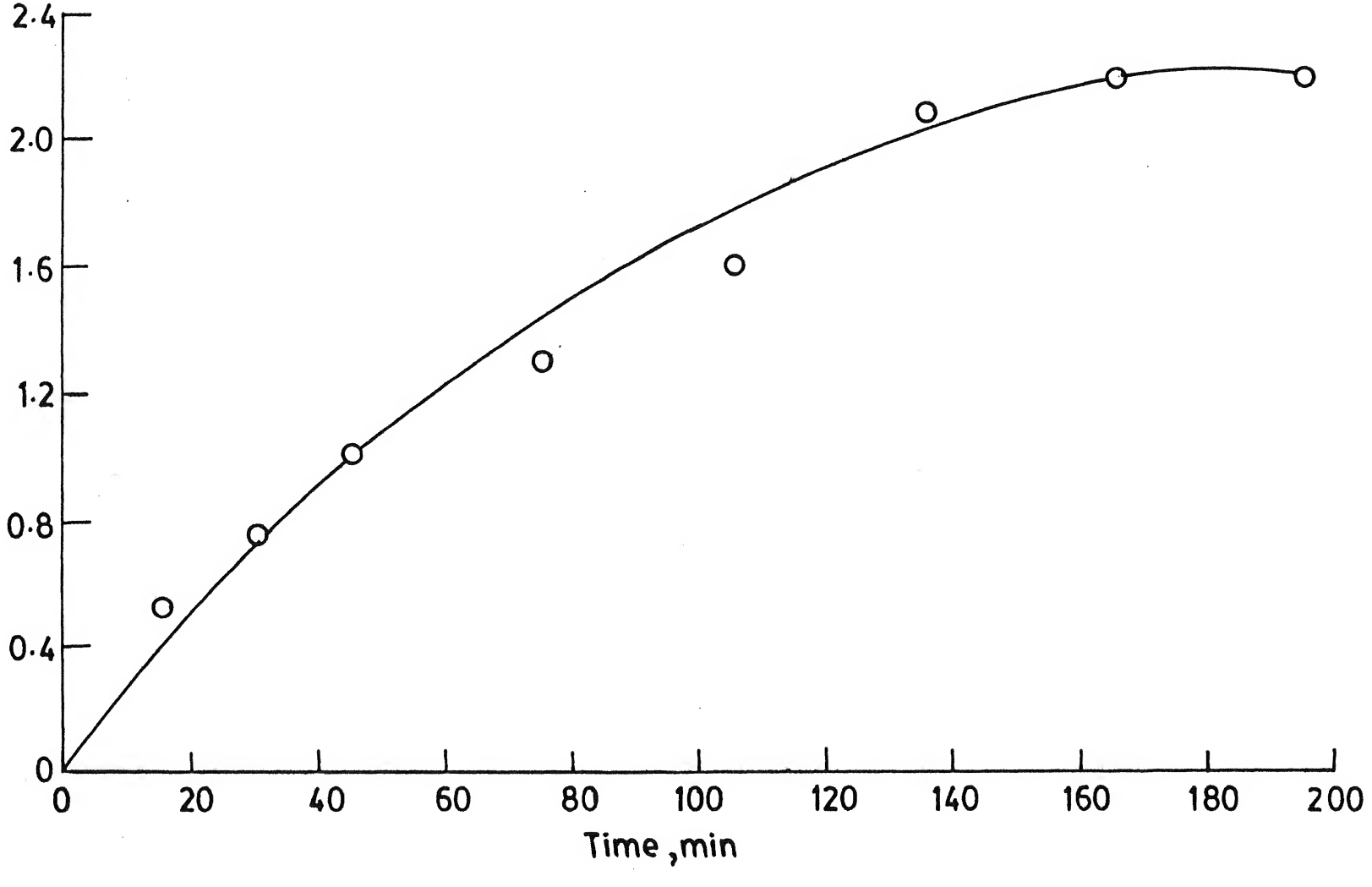

FIG. 13 TRANSIENT BEHAVIOUR OF DRY BED AT L = 1 kg/m² s

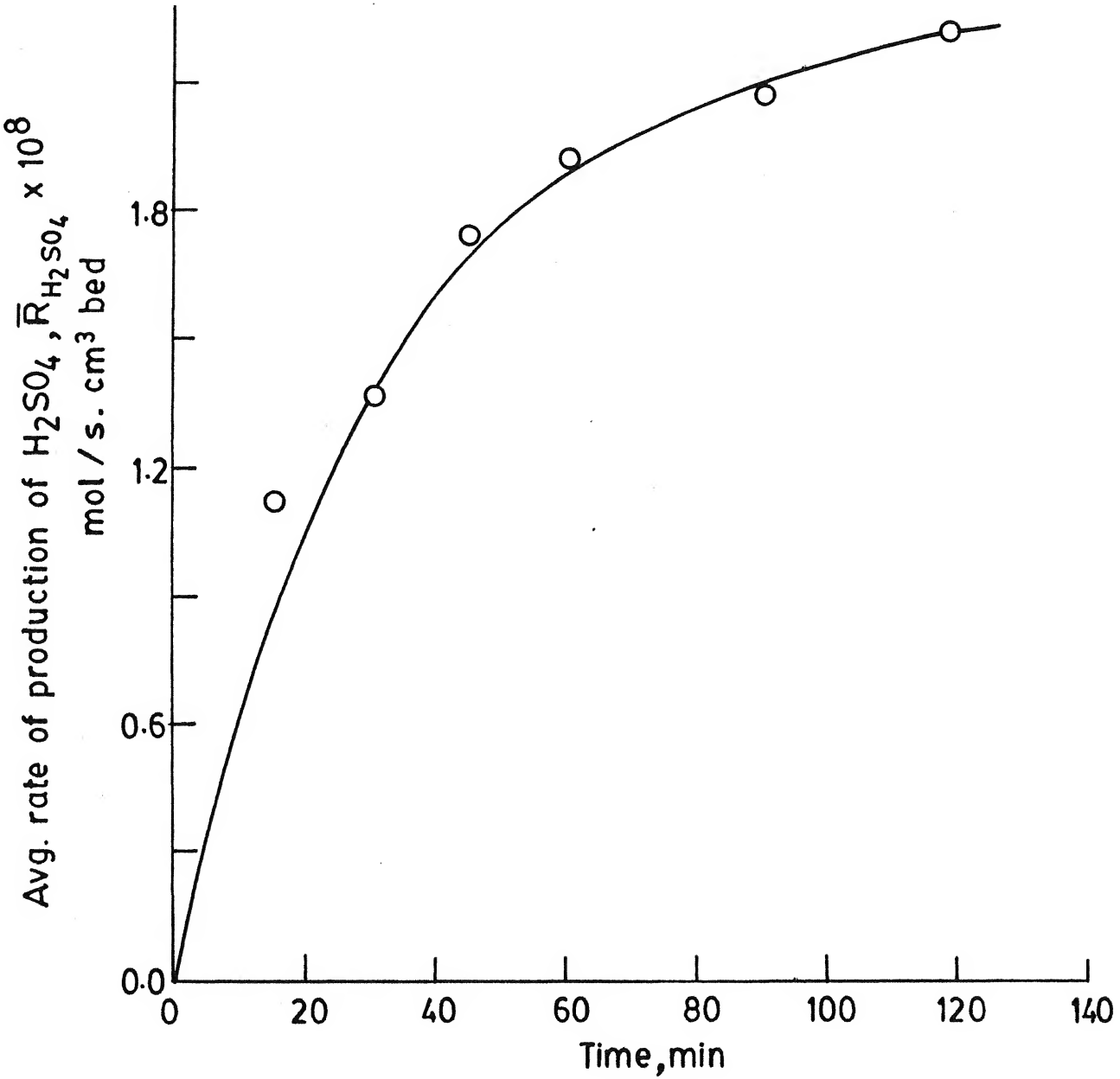
Avg. rate of production of H_2SO_4, $\bar{R}_{H_2SO_4}$ x 10^8
mol / s. cm^3 bed
0.0
0.6
1.2
1.8
0
20
40
60
80
100
120
140
Time, min

liquid flow rate increases both dry and prewetted beds behave similarly. Even the liquid flow distribution was observed to be the same in both cases at high liquid flow rates. Hence the rates are nearly equal at higher flow rate in both modes of operation. This fact is confirmed from the reaction rate measurements at liquid flow rate of 5 kg/m^2-s at which the reaction rates in both the cases are almost equal and the values being in dry mode $1.4x10^{-8}$ and in wet mode $1.58x10^{-8}$. Here also the decrease in rate with increase in flow rate is due to the increase in film thickness.

The above observations from reaction rate measurements reveal that the startup procedure effects the reaction rates in the trickle-bed reactors. At liquid flow rates as low as 1 kg/m^2-s the liquid flow distribution as well as the reaction rates are different for non-prewetted and prewetted modes of operation whereas at high liquid flow rates they behave similar in case of porous particles.

3.6 Reaction Rate Modelling in Prewetted Beds

It was observed from the liquid distribution experiments that the gas and liquid flow throughout the bed in the case of prewetted mode of operation. Precisely, the liquid flows as film over the catalyst particles and the gas flows over the liquid film. The thickness of the film depends upon the liquid flow rate of operation. The film flow prevailing throughout the bed in the case of prewetted mode of operation covers the external surface of the catalyst particles completely at all liquid flow rates. Hence in case of prewetted mode of operation the fraction of outer

surface of particles covered by liquid is equal to one because of the complete wetting of the external surface of catalyst particles by a liquid, throughout the bed.

In this section a model has been developed to fit the experimental rate data, obtained in prewetted mode of operation.

The catalytic oxidation of sulfur dioxide on activated carbon in the presence of liquid water has been chosen as a model reaction for studying the performance of the trickle-bed reactors. The reaction scheme for the above reaction system is as follows:

$$SO_2(g) + \frac{1}{2} O_2(g) + H_2O(l) \longrightarrow H_2SO_4(l) \qquad (3.1)$$

The limiting reactant in this reaction system is oxygen, which is sparingly soluble in water.

3.7 Model Development

The model equations for oxygen in the gas and liquid phases are developed as follows:

Assumptions:

(1) The pores of the catalyst particles are completely filled with liquid.

(2) The external surface of the catalyst particles has been completely covered with the flowing liquid.

(3) Liquid and gas are distributed uniformly across the bed.

(4) The experimental system was operated under isothermal conditions.

With these assumptions, the following equations are written for the mass balance of oxygen:

In the gas phase:

$$D_g \frac{d^2C_g}{dz^2} - V_g \frac{dC_g}{dz} - K_L a_L \left(\frac{C_g}{H} - C_L \right) = 0 \qquad (3.2)$$

In the liquid phase:

$$D_L \frac{d^2C_L}{dz^2} - V_L \frac{dC_L}{dz} + K_L a_L \left(\frac{C_g}{H} - C_L \right) - k_{Ls} a_{Ls} \left(C_L - C_{i,r_o} \right) = 0 \qquad (3.3)$$

The rate of transfer of oxygen from liquid to particle is equal to the rate of reaction on the liquid-covered surface:

$$k_{Ls} a_{Ls} \left(C_L - C_{i,r_o} \right) = \eta k (1-\varepsilon) \left(C_i \right)_{r_o} \qquad (3.4)$$

The associated boundary conditions are

$$V_g C_{g,0} = V_g C_g - D_g \frac{dC_g}{dz} \qquad \text{at } z = 0 \qquad (3.5)$$

$$V_L C_{L,0} = V_L C_L - D_L \frac{dC_L}{dz} \cancel{- D_L \frac{dC_L}{dz}} \qquad \text{at } z = 0 \qquad (3.6)$$

$$\frac{dc_g}{dz} = 0 \qquad \text{at} \quad z = L \tag{3.7}$$

$$\frac{dc_L}{dz} = 0 \qquad \text{at} \quad z = L \tag{3.8}$$

Equations 3.2 to 3.8 can be solved for the concentration of oxygen in the effluent gas and liquid streams. However, axial dispersion in the gas phase of trickle-bed reactors is probably negligible. And also in most instances axial dispersion is unimportant in the liquid. By neglecting the axial dispersion in the above equations, the equations 3.2 and 3.8 are solved for the effluent concentrations in dimensionless form which is given by (Mata and Smith, 1981).

$$c_g^* = \frac{\left(\theta_f - \mu_2\right) \exp\left(\mu_1\right) - \left(\theta_f - \mu_1\right) \exp\left(\mu_2\right)}{\mu_1 - \mu_2} \tag{3.9}$$

$$c_L^* = \frac{\left(\theta_f - \mu_2\right) \left(\mu_1 + Da_g\right) \exp\left(\mu_1\right)}{\left(\mu_1 - \mu_2\right) Da_g} - \frac{\left(\theta_f - \mu_1\right) \left(\mu_2 + Da_g\right) \exp\left(\mu_2\right)}{\left(\mu_1 - \mu_2\right) D_{ag}} \tag{3.10}$$

where

$$c_g^* = c_g / c_{g.0} \tag{3.11}$$

$$C_L^* = HC_L/C_{g,0} \tag{3.12}$$

$$\mu_1,\mu_2 = \frac{1}{2}\left\{-\xi \pm \left|\xi^2 + 4\ Da_g\ Da_L\left(1 - \frac{1}{\eta_{of}}\right)\right|^{1/2}\right\} \tag{3.13}$$

$$\xi = Da_g + \frac{Da_L}{\eta_{of}} \tag{3.14}$$

$$\eta_{of} = \left[1 + \frac{\eta\ k\ \eta_{Ls}(1-\varepsilon)}{K_L\ a_L}\right]^{-1} \tag{3.15}$$

$$\eta_{Ls} = \left[1 + \frac{\eta\ k\ (1-\varepsilon)}{K_{Ls}\ a_{Ls}}\right]^{-1} \tag{3.16}$$

$$\theta_f = Da_g\left(C_{L,0}^* - 1\right) \tag{3.17}$$

$$Da_g = K_L\ a_L\ L/H\ V_g \tag{3.18}$$

$$Da_L = K_L\ a_L\ L/V_L \tag{3.19}$$

The rate of oxygen consumed, $-R_{o_2}$, V_R in the whole reactor is related to the effluent concentrations by an overall oxygen

balance:

$$R_{o_2} V_R = \frac{Q_L C_{g,0}}{H} \left(C^*_{L,0} - C^*_{L,L}\right) + Q_g C_{g,0}\left(1 - C^*_{g,L}\right) \qquad (3.20)$$

The above equation can be rearranged in terms of the rate of formation of sulfuric acid.

$$\bar{R}_{H_2SO_4} = \frac{2}{\bar{V}_R}\left[\frac{Q_L C_{g,0}}{H}\left(C^*_{L,0} - C^*_{L,L}\right) + Q_g C_{g,0}\left(1 - C^*_{g,L}\right)\right] \qquad (3.21)$$

The parameters $K_L a_L$ and $K_{Ls} a_{Ls}$ can now be estimated from the above equations for the measured reaction rates.

Komiyama and Smith (1975) have studied the intrinsic kinetics of the sulfur dioxide oxidation using BPL-type activated carbon. They observed that the rate is zero order in SO_2 and first order in oxygen in a slurry reactor. They reported a value of 0.14 s^{-1} for $k\eta$. Since this study also utilized the same type of carbon particles, the same value of $k\eta = 0.14\ s^{-1}$ has been assumed in the analysis of the reaction rate data. The rate expression developed in eqn. 3.21 has been utilized in estimating the mass transfer coefficients. The parameters were estimated using Marquardt's nonlinear least squares algorithm. The results are shown in Table 3.3 and in Fig.15 and Fig.16.

As expected, $K_{Ls} a_{Ls}$ is a strong function of liquid flow rate and is increasing with increase in liquid flow rate. However, liquid flow rate has a little influence on $K_L a_L$. The mass transfer coefficients estimated are higher than the mass transfer coefficients from Goto and Smith (1975) correlation. However, as

Table 3.3

Predicted Mass Transfer Coefficients from Proposed Model

Superficial liquid velocity (cm/s)	$K_L a_L$ (s^{-1})	$k_{Ls} a_{Ls}$ (s^{-1})
0.16	0.0096	0.0607
0.26	0.0098	0.0869
0.35	0.012	0.1079
0.44	0.014	0.1241
0.56	0.015	0.1468

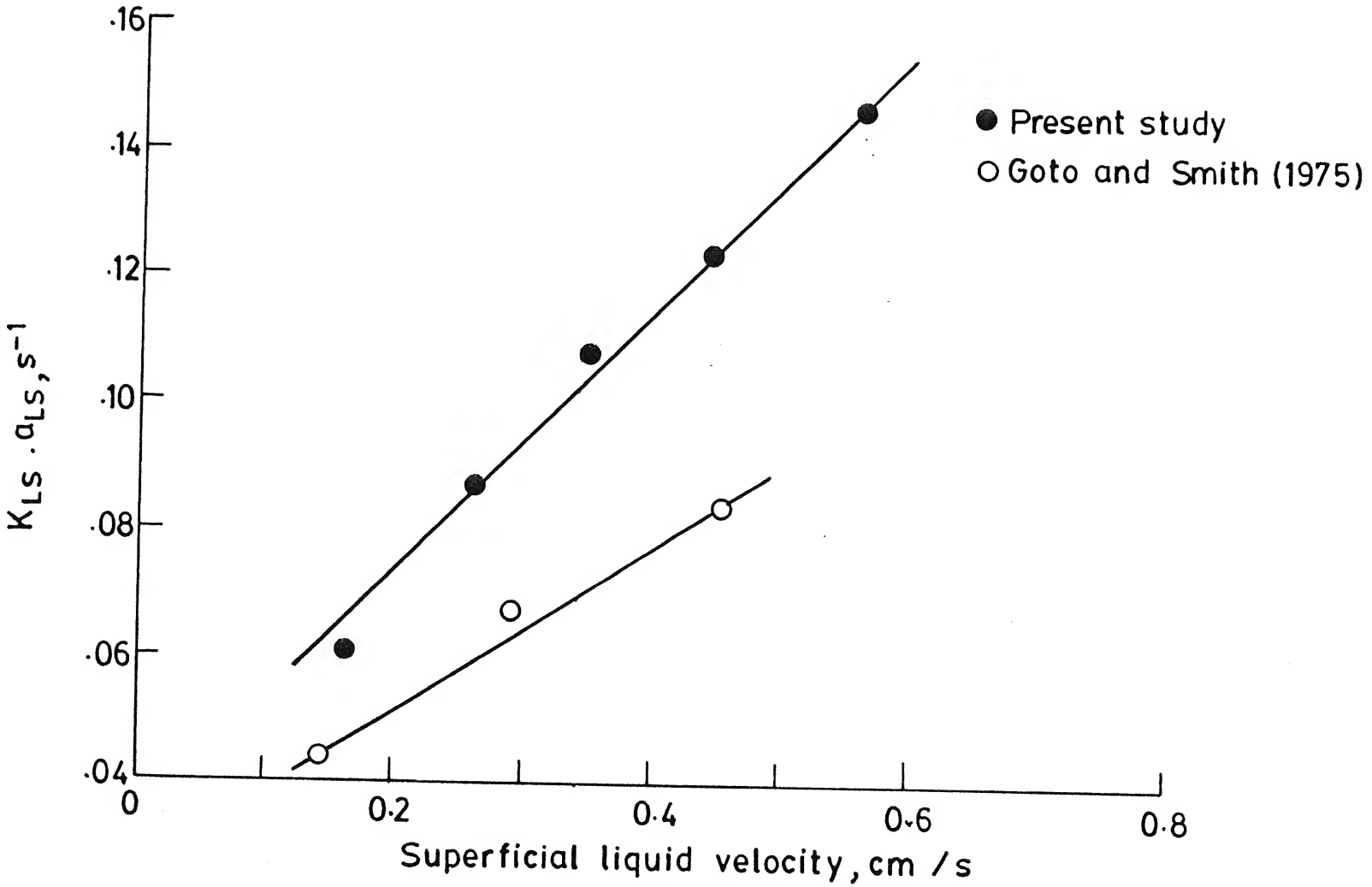

FIG. 15 PREDICTED LIQUID TO SOLID MASS TRANSFER COEFFICIENTS

it has been demonstrated by Turek and Lange (1981), that in the presence of reaction, enhancement of mass transfer rates occurs. Hence, the present model can explain the observed reaction rate trends in trickle-bed reactors.

CHAPTER 4

CONCLUSIONS AND RECOMMENDATIONS FOR FUTURE WORK

4.1 Conclusions

At low liquid flow rates the liquid flow distribution was found to depend on startup procedure viz., prewetted and non-prewetted beds. In case of non-prewetted beds at very low liquid flow rates in the range of 0.5-1 kg/m^2-s, 20% of the bed was found to be occupied with dry zones. The liquid flow through the rest of the bed being predominantly filament flow.

In case of prewetted beds, it was observed that the liquid is flowing throughout the bed cross-section, the flow over the catalyst particles being predominantly film flow.

The liquid flow distribution in case of prewetted beds was observed to be more uniform compared to that in non-prewetted beds at low liquid flow rates ($L < 1$ kg/m^2-s). However, at high liquid flow rates ($L < 1$ kg/m^2-s) the liquid flow distribution was found to be similar in both prewetted and non-prewetted beds.

In non-prewetted beds the hydrodynamic steady state reached in about 2h whereas in prewetted beds at ($L < 1$ kg/m^2-s) the steady state attained in 15 minutes from the start of the run.

The reaction rates at low liquid flow rates ($L < 1$ kg/m^2-s) were found to depend on the startup procedure. In prewetted bed mode of operation the reaction rates were found to decrease with increase in liquid flow rate. In dry beds it is observed that at ($L < 1$ kg/m^2-s), the reaction rates are 40% less than that in prewetted bed. With the increase in liquid flow

rates beyond 1 kg/m^2-s, the reaction rates in non-prewetted beds approached those observed in prewetted bed for the same liquid flow rate.

Finally, a model has been proposed to fit the experimental data obtained in prewetted beds. The model parameters, viz., gas-liquid and liquid-solid mass transfer coefficients were estimated from the experimental data assuming complete wetting of the catalyst particles.

4.2 Recommendations for future work

1. The effect of particle diameter on liquid flow distribution and reaction rate measurements can be studied by employing different particle sizes.
2. Herskowitz and Mosseri (1983) have demonstrated that the gas flow rate has a significant effect on the reaction rates in the study of hydrogenation of alpha methyl styrene. Therefore, the effect of gas flow rate on the reaction rates can also be studied.
3. The liquid flow distribution depends upon the way in which the liquid has been introduced into the reactor. Hence, the reaction rate studies with different liquid inlet configurations viz., single inlet, line inlet etc., can also be studied.
4. It is expected to observe minima in the reaction rate curve with saturated liquid feeds. Hence, the reaction rate measurements can also be made with saturated liquid feeds.

NOMENCLATURE

a_L gas-liquid mass transfer, $cm^2/(cm^3$ of reactor).

a_{Ls} liquid-particle mass transfer area, $cm^2/(cm^3$ of reactor).

C concentration of oxygen mol/cm^3; subscript i denotes intraparticle (pore) region, g denotes bulk gas, L bulk liquid.

$(C_{i,L})_{r0}$ concentration in the liquid at the outer surface of the particle mol/cm^3.

$C_{g,0}$ concentration in the gas feed, mol/cm^3.

$C_{L,0}$ concentration in the liquid feed, mol/cm^3.

C_g^* $=C_g/C_{g,0}$, dimensionless gas concentration.

C_L^* $=HC_L/C_{g,0}$, dimensionless liquid concentration

d_p particle diameter, cm

D_g, D_L axial dispersion coefficients in the gas and liquid phases, cm^2/s.

Da_g, Da_L K_La_LL/Hv_g, K_La_LL/v_L, Damköhler numbers based upon gas and liquid flow rates.

H $=(C_g/C_L)_{equil}$, Henry's law constant for oxygen in water.

k intrinsic first-order rate constant based upon a unit volume of particles, s^{-1}.

k_{Ls} liquid-particle mass transfer coefficient on the liquid-covered surface cm/s.

K_L overall gas-to-liquid mass transfer coefficient, cm/s.

L catalyst bed depth, cm

Q volumetric flow rate, cm^3/s

r_o radius of particle, cm

$\bar{R}_{H_2SO_4}$ rate of production of H_2SO_4 in the reactor (average rate), mol/s (cm^3 of reactor).

R_{O_2} global rate of reaction of oxygen, mol/s (cm^3 of reactor).

v superficial fluid velocity, cm/s.

V_R reactor volume (empty), cm^3.

z axial coordinate in reactor, cm.

Greek symbols

ε void fraction in the bed

η effectiveness factor

~~factor~~

η_{Ls} liquid-particle effectiveness factor

~~effectiveness factor~~,

eqn.(3.16).

η_{of} overall effectiveness factor, eqn.(3.15).

θ_f, ξ auxiliary variables defined by eqns.(3.17) and (3.14).

μ_1, μ_2 roots, defined by eqn.(3.13), of characteristic equation for the solution of the differential mass conservation equations.

Subscripts

g,L gas and liquid phases.

Superscript

* denotes dimensionless quantity.

REFERENCES

1. Ahtchi-Ali, B., and H. Pedersen, "Very Large Lattice Model of Liquid Mixing in Trickle-Beds," Ind. Eng. Chem. Fund., 25, 108 (1986).

2. Bemer, G.G., and F.J. Zuiderweg, "Radial Liquid Spread and Maldistribution in Packed Columns Under Different Wetting Conditions, " Chem. Eng. Sci., 33, 1637 (1978).

3. Berruti, F., R.R. Hudgins, E. Rhodes and S. Sicardi, "Oxidation of Sulfur Dioxide in a Trickled-Bed Reactor," Can. J. Chem. Eng. 62, 644 (1984).

4. Christensen, G., S.J. McGovern, and S. Sundaresan, "Cocurrent Downflow of Air and Water in Two-Dimensional Packed Column," AIChE J., 32, 1677 (1986).

5. Gianetto, A. and P.L. Silveston, "Multiphase Chemical Reactors - Theory, Design and Scale-up," Hemisphere Publ. Corp., Washington, D.C., (1986).

6. Hartman, M. and R.W. Coughlin, "Oxidation of SO_2 in a Trickle-Bed Reactor Packed with Carbon," Chem. Eng. Sci. 27, 867 (1972).

7. Haure, P.M., R.R. Hudgins and P.L. Silveston, "Periodic Operation of a Trickle-Bed Reactor," AIChE J. 35, 1437 (1989).

8. Haure, P.M., R.R. Hudgins and P.L. Silveston, "Investigations of SO_2 Oxidation Rates in Trickle-Bed Reactors Operating at Low Liquid Flow Rates," Can. J. Chem. Eng. 70, 600 (1992).

9. Herskowitz, M., and J.M. Smith, "Liquid Distribution in Trickle-Bed Reactors," AIChE J., 24, 439 (1978).

10. Herskowitz, M. and S. Mosseri, "Global Rates of Reaction in Trickle-Bed Reactors: Effect of Gas and Liquid Flow Rates," Ind. Eng. Chem. Fund. 22, 4 (1983).

11. Komiyama, H. and N.M. Smith, "Sulfur Dioxide Oxidation in Slurries of Activated Carbon, Part I Kinetics," AIChE J., 21, 664 (1975).

12. Lazzaroni, C.L., H.R. Keselman, and N.S. Figoli, "Colorimetric Evaluation of the Efficiency of Liquid-Solid Contacting in Trickle Flow," Ind. Eng. Chem. Res., 27, 1132 (1988).

13. Lutran, P.G., K.M. Ng and E.P. Delikat, "Liquid Distribution in Trickle-Beds. An Experimental Study Using Computer-Assisted Tomography," Ind. Eng. Chem. Res., 30, 1270 (1991).

14. Marchot, P., M. Crine, and G.A.L. Homme, "Rational Description of Trickle Flow through Packed Beds. Part-I: Liquid Distribution Far from the Distributor," Chem. Eng. J., 48, 49 (1992).

15. Mata, A.R., and J.M. Smith, "Oxidation of Sulfur Dioxide in a Trickle-Bed Reactor," Chem. Eng. J. 22, 229 (1981).

16. Melli, T.R., J.M. de Santos, W.B. Kolb and L.E. Scriven, "Cocurrent Downflow in Networks of Passages. Microscopic Roots of Macroscale Flow Regimes," Ind. Eng. Chem. Res., 29, 2367 (1990).

17 Mellor, J.W.,"Modern Inorganic Chemistry", McGraw Hill, NY (1956).

18. Pavko, A. and J. Levec, "Wetting Efficiency in a Trickle-Bed Reactor," Proc. 2nd World Congr. Chem. Eng., Montreal, Vol. III, 156 (1981).

19 Ramachandran, P.A., and R.V. Chaudhari, "Three-Phase Catalytic Reactors," Gordon and Breach Science Publishers, NY (1983).

20. Sattterfield,C.N. and F. Ozel, "Direct Solid-Catalyzed Reaction of a Vapor in an Apparently Completely Wetted Trickle Bed Reactor," AIChE J., 19, 1259 (1973).

21. Sedricks, W. and C.N. Kenney, "Partial Wetting in Trickle-Bed Reactors," Chem. Eng. Sci., 28, 558 (1973).

22. Vogel's Text Book of Quantitative Chemical Analysis, 5th Edn., ELBS, London (1989).

APPENDIX A

Procedures for Preparation and Standardization of reagents titrimetric analysis

A.1 Preparation of Standard 0.1N Potassium Iodate Solution

1. Dry the potassium iodate at 120°C for 1 hr and cool it i covered vessel in a desiccator.
2. Weigh out 3.566 g KIO_3 on a watch glass.
3. Transfer KIO_3 to 1 lit. volumetric flask.
4. Add about 400-500 cc of water and gently rotate the flask ur the salt is completely dissolved.
5. Make up to the mark with distilled water. Shake well.

A.2. Preparation of 0.1 N Iodine Solution

1. Dissolve 20g of iodate-free potassium iodide in 30-40 cc water in 1 lit. volumetric flask.
2. Take 12.7 g of A.R. grade iodine and add this to the ab potassium iodide solution.
3. Close the stopper of the volumetric flask and shake the fl until all the iodine is dissolved.
4. Leave the solution to acquire room temperature.
5. Add distilled water to make the volume to 1 lit.

A.3 Preparation of 0.1 N Sodium Thiosulphate Solution.

1. Weigh out 25 g. sodium thiosulphate crystals $Na_2S_2O_3.5H_2O$ dissolve in distilled water.

2. Make the volume of the solution to 1 litre with boiled distilled water.
3. Add 3 drops of chloroform or 0.1 g. sodium carbonate to st the solution for more than few days.

A.4 Standardisation of Sodium Thiosulphate Solution

1. Take 25 cc of the KIO_3 solution.
2. Add 1 gm. of iodate free Potassium Iodide.
3. Add 1 cc of 1M-sulfuric acid.
4. Titrate this solution (liberated iodine) with the thiosulph solution with constant shaking when the color of the liquid become pale yellow.
5. Add 200 cc distilled water.
6. Add 2 cc of starch solution.
7. Continue the titration until the color changes from blue colorless.

A.5 Standardisation of Iodine Solution

1. Take 25 cc iodine solution to 250 cc conical flask.
2. Add 75 cc distilled water.
3. Add the standard sodium thiosulphate solution from a buret until the solution has a pale-yellow color.
4. Add 2 cc starch solution.
5. Continue the addition of the thiosulphate solution slowly unt the solution is colorless.

A.6 Estimation of dissolved SO_2 in the liquid

a. Pipette 25 cc of 0.1 N iodine solution into 250 cc conical flask.

b. Add 5 cc 2M-hydrochloric acid.

c. Add 150 cc distilled water.

d. Take 20 cc of sample (reactor outlet liquid) and slowly add this solution from a burette with constant stirring with the jet close to the surface of the liquid.

e. Titrate this solution with 0.1 N sodium thiosulphate

(i) Add the sodium thiosulphate solution from a burette until the solution has a pale-yellow color.

(ii) Add 2cc of starch solution and continue the addition of the thiosulphate solution slowly until the solution is just colorless.

A.7 Preparation of Standard 0.1N Potassium Hydrogen Pthalate Solution

a. 5.1 g of pure potassium hydrogen phthalate is accurately weighted.

b. The weighted material is transferred to 250 ml graduated flask.

c. Distilled water is added to make the solutions to the mark.

A.8 Preparation of 0.1N NaOH solution

a. 4.2 g of sodium hydroxide is weighted.

b. The weighted material is transferred to 100 ml flask.

c. Boiled out distilled water is added to the flask upto the

mark to make the solution to 1 lit.

A.9 Standardization of NaOH solutions

a. Take 25 ml of standard 0.1N potassium hydrogen phthalate in a conical flask.

b. Add 2-3 drops of phenolphthalein.

c. The solution is titrated with the sodium hydroxide solution contained in a burette.

A.10 Estimation of H_2SO_4 in liquid sample after 10 min. of boiling

a. 100 ml of the liquid sample is taken in a conical flask.

b. 2-3 drops of phenolphthalein is added to the liquid sample.

c. The solution is titrated against the standard sodium hydroxide solution contained in a burette.